

pH-Tuned metal coordination and peroxidase activity of a peptide dendrimer enzyme model with a Fe(II)-bipyridine at its core

Piero Geotti-Bianchini, Tamis Darbre* and Jean-Louis Reymond*

*Department of Chemistry and Biochemistry, University of Berne,
Freiestrasse 3, CH-3018 Berne, Switzerland*

Correspondence to: jean-louis.reymond@ioc.unibe.ch; tamis.darbre@ioc.unibe.ch

SUPPORTING INFORMATION

Content

Reagents and materials.....	S2
Instruments and characterization techniques.....	S2
Synthesis and characterization.....	S3
HPLC, UPLC and MS data of peptide dendrimers.....	S4
Metal binding tests.....	S12
Data fitting procedure.....	S12
Spectrophotometric titrations and titration curve fittings.....	S13
Characterization of the metal complexes.....	S17
HPLC comparison of bipyridine dendrimer ligands and their metal complexes.....	S17
Reversibility of the stoichiometric change in Fe(II) complexation upon pH switch.....	S18
Determination of the apparent pK _a	S19
BP1/BP4 mixed Fe(II) complex.....	S20
NMR diffusion measurements.....	S23
CD measurements.....	S30
Catalytic assays.....	S31
Determination of the amount of oxidized substrate.....	S31
Test of oxidation catalysis.....	S33
Data treatment.....	S34
References.....	S37

Reagents and materials

Dichloromethane (DCM) and methanol (MeOH) for solid phase peptide synthesis (SPPS) were freshly distilled before use. Acetonitrile (MeCN) was HPLC grade. Fmoc-protected amino acids, including 4-aminomethyl-benzoic acid (Amb) were purchased from Novabiochem. All other reagents were analytical grade or higher and were used without further purification. Air sensitive reactions were performed under argon.

Instruments and characterization techniques

Analytical chromatograms were acquired on a Water 600 HPLC equipped with a Waters Atlantis dC18 (4.6 x 100 mm², 5 µm, 120 Å) column (flow 1.2 mL/min) and a Waters 960 PDA detector (λ 190-700 nm) or on a Dionex Ultimate 3000 RS UPLC equipped with an Acclaim RSLC 120 C18 (50 x 3.0 mm², 2.2 µm, 120 Å) column (flow 1.2 mL/min) and a Dionex Ultimate 3000 RS diode array detector (λ 190-400 nm).

Preparative HPLC purifications were performed on a Waters Prep LC Controller instrument equipped with a Waters Atlantis Prep T3 OBD (100 x 30 mm², 5 µm, 100 Å) column and a Waters 2489 UV-detector monitoring at λ 214 nm as well as a with a Goerz Servogr 120 paper recorder. milliQ H₂O + 0.1 % TFA (A) and MeCN + 0.1 % TFA (B) were used as eluents.

ESI-MS spectra were acquired on a Thermo Scientific LTQ Orbitrap or on an Applied Biosystem AB2000 Q-Trap spectrometer instrument. ESI(+) samples were diluted in H₂O/MeCN 1:1 + 1 % formic acid, ESI(-) samples were diluted in H₂O/MeCN 1:1 + 1 % triethylamine. MALDI-MS spectra were acquired on an Applied Biosystems Voyager Elite spectrometer using a 3,5-dimethoxy-4-hydroxycinnamic acid (sinapinic acid) or a α-cyanocinnamic acid matrix.

NMR spectra were acquired on a Bruker Avance 300 MHz instrument, NMR diffusion experiments were performed on a Bruker Avance 400 MHz instrument.

UV-Vis spectra were acquired on a Varian Cary 100 Bio spectrophotometer equipped with a Varian Temperature Controller thermostat.

CD spectra were measured on a Jasco J-715 spectropolarimeter equipped with a Haake FS thermostat controlled by a Jasco PFD 350S device.

A SpectraMax250 (Molecular Devices) 96-well microtiter plate reader was used for the microtiter plate assays, including the catalytic experiments.

Synthesis and characterization

5,5'-Bis(hydroxymethyl)-2,2'-bipyridine [bipy(CH₂OH)₂]

5,5'-di-(ethoxycarbonyl)-[2,2']bipyridine (0.258 g, 0.86 mmol, prepared according to the literature[S1]) was dissolved in 4.4 mL anhydrous THF under Ar. The mixture was cooled to -78°C in an acetone/CO₂(s) bath, then 1 M LiAlH₄ in THF (1.75 mL, 1.75 mmol) was added. The heterogeneous mixture was stirred and allowed to warm up to -20°C. After 30 min, the mixture was cooled again to -78°C and 2.7 mL 4:1 H₂O/THF mixture were added slowly. The mixture was allowed to warm up to room temperature, then celite was added and the mixture was stirred for further 15 min at room temperature. The solid was filtered and washed with THF. The yellow filtrate was concentrated at reduced pressure, then dried under high vacuum overnight, yielding 0.150 g (0.69 mmol, 82 %) of the title compound as a reddish waxy solid, which was used in the next step without further purification.

R_f: 0.23 (DCM:MeOH 9:1). MS (ESI⁺): Calcd for C₁₂H₁₃N₂O₂: *m/z* 239.08, Found *m/z* 239.1 ([M+H]⁺).

¹H-NMR (CDCl₃, 300 MHz), δ/ppm: 8.67 (s br, 2H, 2 C(6)H bipy), 8.40-8.37 (d, *J*= 8.4 Hz, 2H, 2 C(3)H bipy), 7.87-7.83 (dd, *J*= 2.1, 8.2 Hz, 2H, C(4)H bipy), 4.81 (s, 4H, 2 CH₂), 1.44 (s, 2H, 2 OH).

5,5'-Bis(bromomethyl)-2,2'-bipyridine [1]

10 mL MeCN/DCM 1:1 were added to crude bipy(CH₂OH)₂ (0.15 g, 0.69 mmol) and the mixture was extensively sonicated. Dry DMF was added dropwise until complete dissolution. PPh₃ (0.422 g, 1.56 mmol) was added and after complete dissolution of the resulting suspension, *N*-bromosuccinimide (0.296 g, 1.61 mmol) was added. The mixture turned latescent, then clear and dark orange. After stirring for further 2 h with exclusion of moisture, insoluble matter was filtered out, the bright orange filtrates were concentrated under reduced pressure to an oily orange solid, which was purified by flash-chromatography (*n*-hexane/AcOEt 1:1), yielding 0.095 g (0.28 mmol, 37 %) of the title compound as a pale yellow solid.

R_f: 0.24 (*n*-hexane/AcOEt 1:1). HR-MS (ESI⁺): Calcd for C₁₂H₁₁N₂Br₂: *m/z* 340.9283, Found: *m/z* 340.9301 ([M+H]⁺); Calcd for C₁₂H₁₀N₂Br₂Na: *m/z* 362.9108, Found: *m/z* 362.9122 ([M+Na]⁺).

HPLC (18-60 % B in 10 min): t_r = 8.80 min.

¹H-NMR (CDCl₃, 300 MHz), δ/ppm: 8.69-8.68 (d, *J*= 2.1 Hz, 2H, 2 C(6)H bipy), 8.42-8.39 (d, *J*= 8.4 Hz, 2H, 2 C(3)H bipy), 7.87-7.84 (dd, *J*= 2.2, 8.4 Hz, 2 C(4)H), 4.54 (s, 4H, 2 CH₂Br).

¹³C-NMR (CDCl₃, 76 MHz), δ/ppm: 155.57 (C, C(2) bipy), 149.51 (CH, C(6)H bipy), 137.76 (CH, C(4) bipy), 134.04 (C, C(5) bipy), 121.31 (CH, C(3) bipy), 29.68 (CH₂, CH₂Br).

General SPPS synthesis

Cysteine-containing peptide dendrimers (**N1**, **N2**, **N3**, **N4**) were synthesized on solid-phase employing the Fmoc/*t*Bu strategy. The synthesis was performed manually in polypropylene syringes attached to a rotating axis. The resin Tentagel S Ram, loading 0.24 mmol/g, from Rapp Polymere GmbH was used as a solid support.

The Fmoc-protecting group was removed by treatment with 20 % piperidine in DMF (2 × 10 min).

The general coupling protocol employed 3 eq each of Fmoc-protected amino acid and PyBOP in *N*-methylpyrrolidone and 5 eq of DIEA. Coupling times were of 45 min for residues in the focal point and doubled after each branching unit. Completeness of the coupling and deprotection steps was checked with the trinitrobenzenesulfonic acid (TNBS) test. In case of incomplete coupling/deprotection, the step was repeated. After completion of the peptide sequences, the peptides were Fmoc-deprotected and acetylated with Ac₂O/DCM 1:1 for 1 hour.

Peptide dendrimers were cleaved from the resin by treatment with the cleavage mixture TFA/H₂O/*triisopropylsilane*/1,2-ethanedithiol 94:1:2.5:2.5 (v/v/v/v). The crude products were precipitated with chilled methyl-*tert*butylether, separated from the cleavage solution by centrifugation (10 min at 4000 rpm), redissolved in milliQ H₂O + 0.1 % TFA and lyophilized prior to HPLC purification.

Table S1. Properties of the four Cys-Containing Dendrimers **Nn** (n= 1-4) Employed for the Synthesis of the Bipyridine Peptide Dendrimers **BPn** (n= 1-4)

Nn	Sequence	MS (calc/found)	yield (mg) [%]
N1 ^a	(Ac- ES) ₈ -(ZE A) ₄ -(ZXY) ₂ -ZCD-NH ₂ ^{b,c}	4297.1/4297.0	210 [24]
N2 ^a	(Ac- QS) ₈ -(ZE A) ₄ -(ZXY) ₂ -ZCD-NH ₂ ^{b,c}	4289.3/4289.0	44 [5]
N3 ^a	(Ac- QS) ₈ -(ZQ A) ₄ -(ZXY) ₂ -ZCD-NH ₂ ^{b,c}	4285.4/4286.6	25 [3.6]
N4	(Ac- KS) ₈ -(ZE A) ₄ -(ZXY) ₂ -ZCD-NH ₂ ^{b,c}	4289.6/4289.0	92 [8.6]

^a The synthesis and characterization of **N1**, **N2**, **N3** was already described elsewhere.[S2]

^b X= 4-aminomethyl-benzoic acid, Amb; Z= (*S*)-2,3-diamino-propionic acid (branching unit), Dap. ^c The residues which differ among the four analogues are in bold.

(Ac-Lys-Ser)₈-(Dap-Glu-Ala)₄-(Dap-Amb-Tyr)₂-Dap-Cys-Asp-NH₂ [**N4**]

Synthesis scale: 205 μmol (850 mg resin). After preparative HPLC purification 92.0 mg (17.7 μmol, 8.6 %) of the TFA salt of the title compound **N4** were obtained as a white fluffy solid.

MS(ESI⁺): Calcd for C₁₈₂H₂₈₈N₅₃O₆₅S: *m/z* 4290.62, Found: *m/z* 4291.0 ([M+H]⁺).

UPLC (0-70 % B in 2.2 min): tr 1.462 min.

HPLC, UPLC and MS data of peptide dendrimers

N4

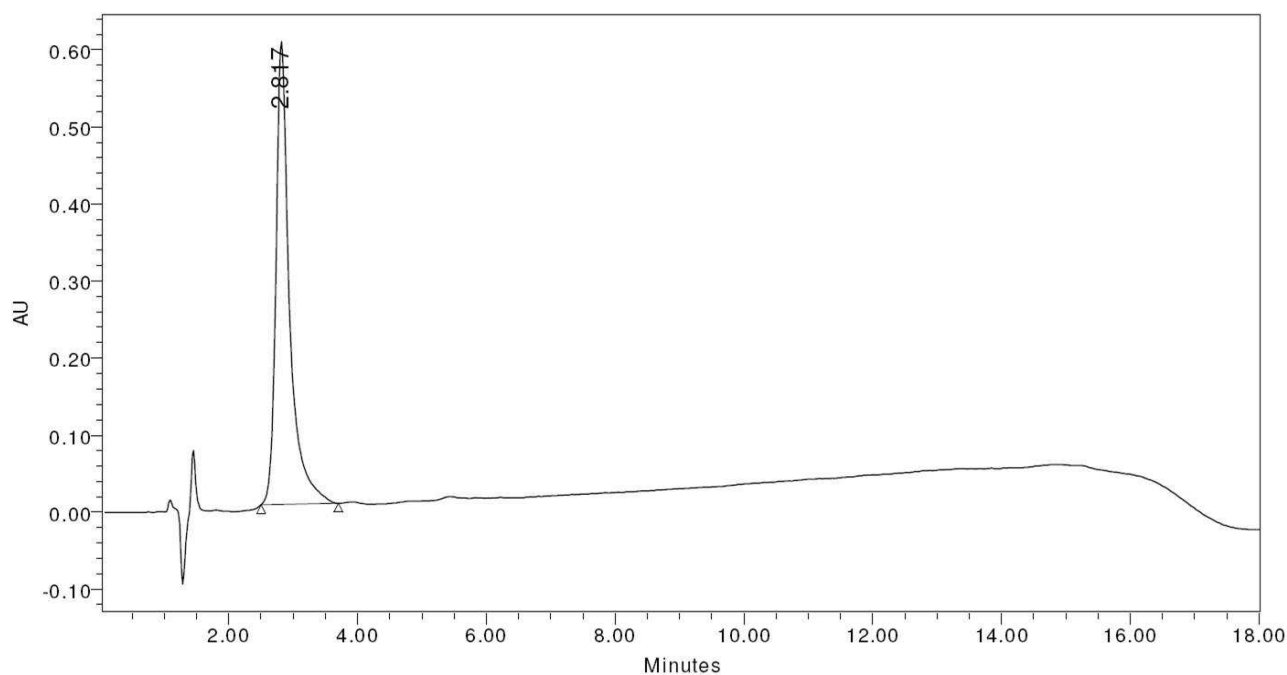


Figure S1. HPLC chromatogram of the purified peptide dendrimer **N4**. Conditions: 18-60 % B in 10 min, λ 214 nm.

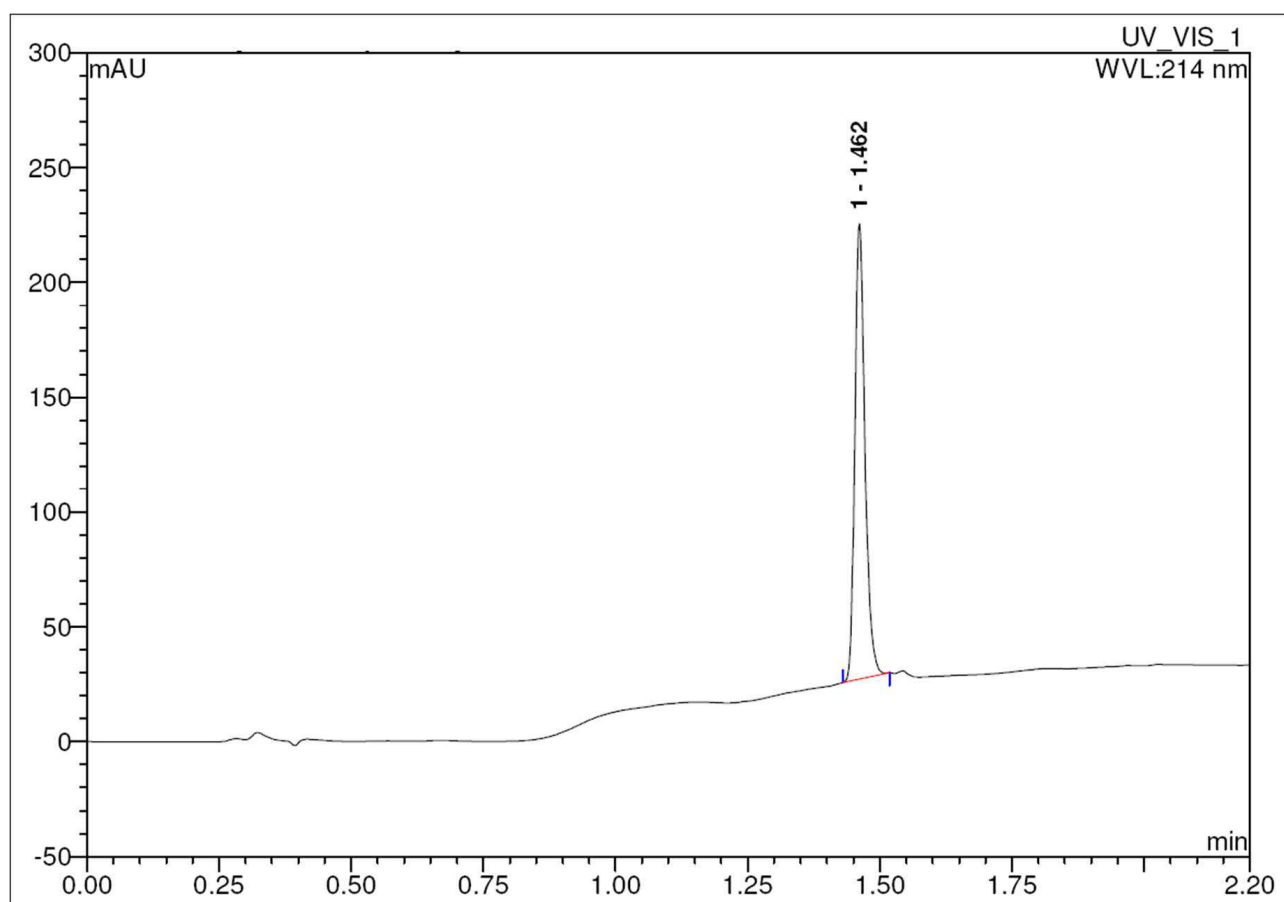


Figure S2. UPLC chromatogram of the purified peptide dendrimer **N4**. Conditions: 0-70 % B in 2.2 min, λ 214 nm.

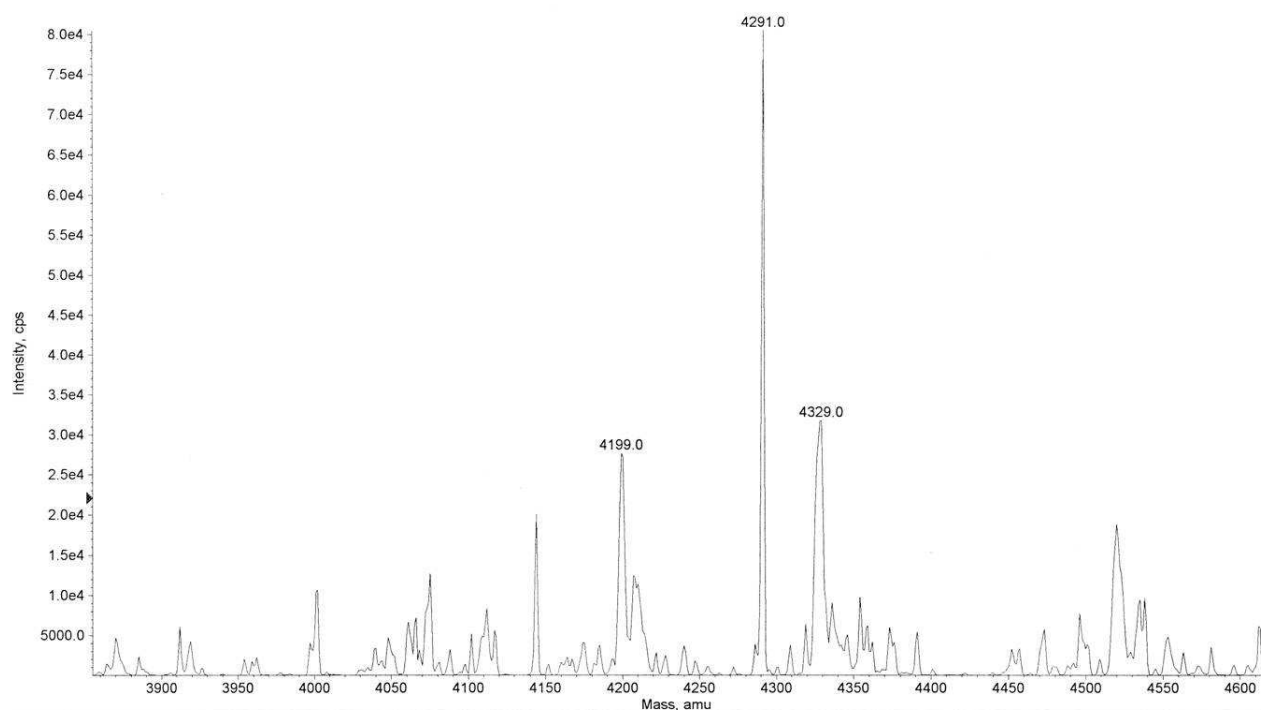


Figure S3. MS reconstruction for the purified peptide dendrimer **N4** (ESI +, AB Q-Trap). m/z 4291.0: $[M+H]^+$, clc 4291.6; m/z 4329.0: $[M+K]^+$, clc 4329.6.

BP1

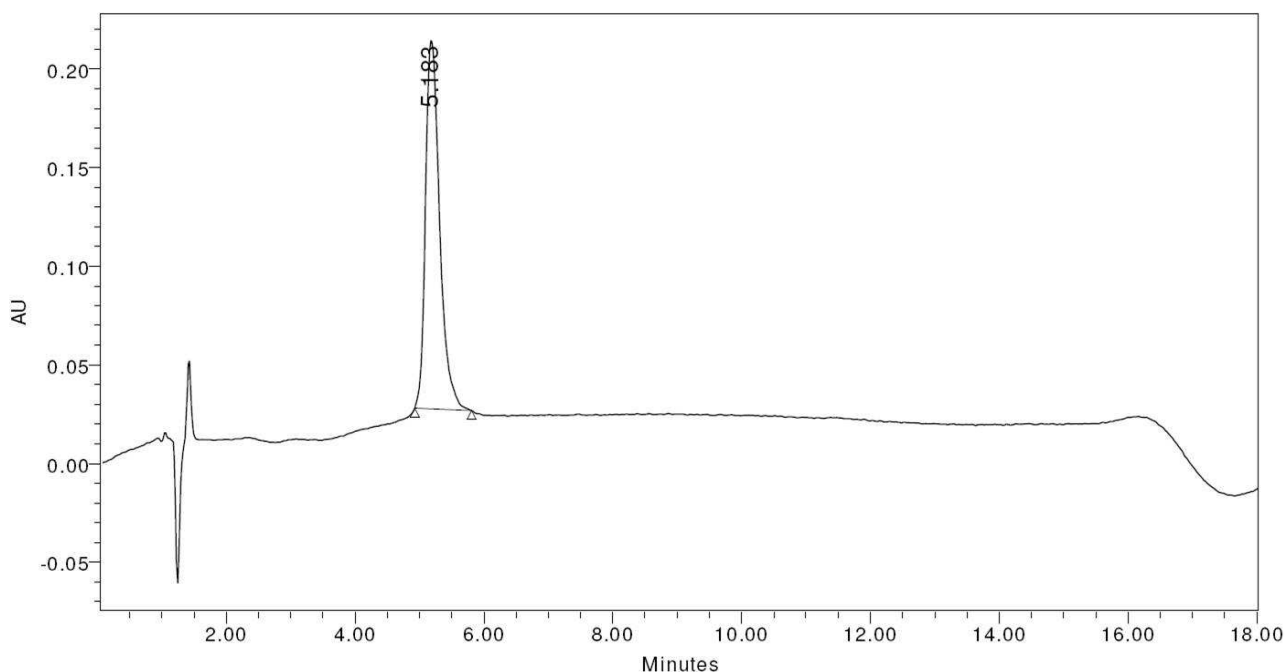


Figure S4. HPLC chromatogram of the purified bipyridine peptide dendrimer **BP1**. Conditions: 18-60 % B in 10 min, λ 214 nm.

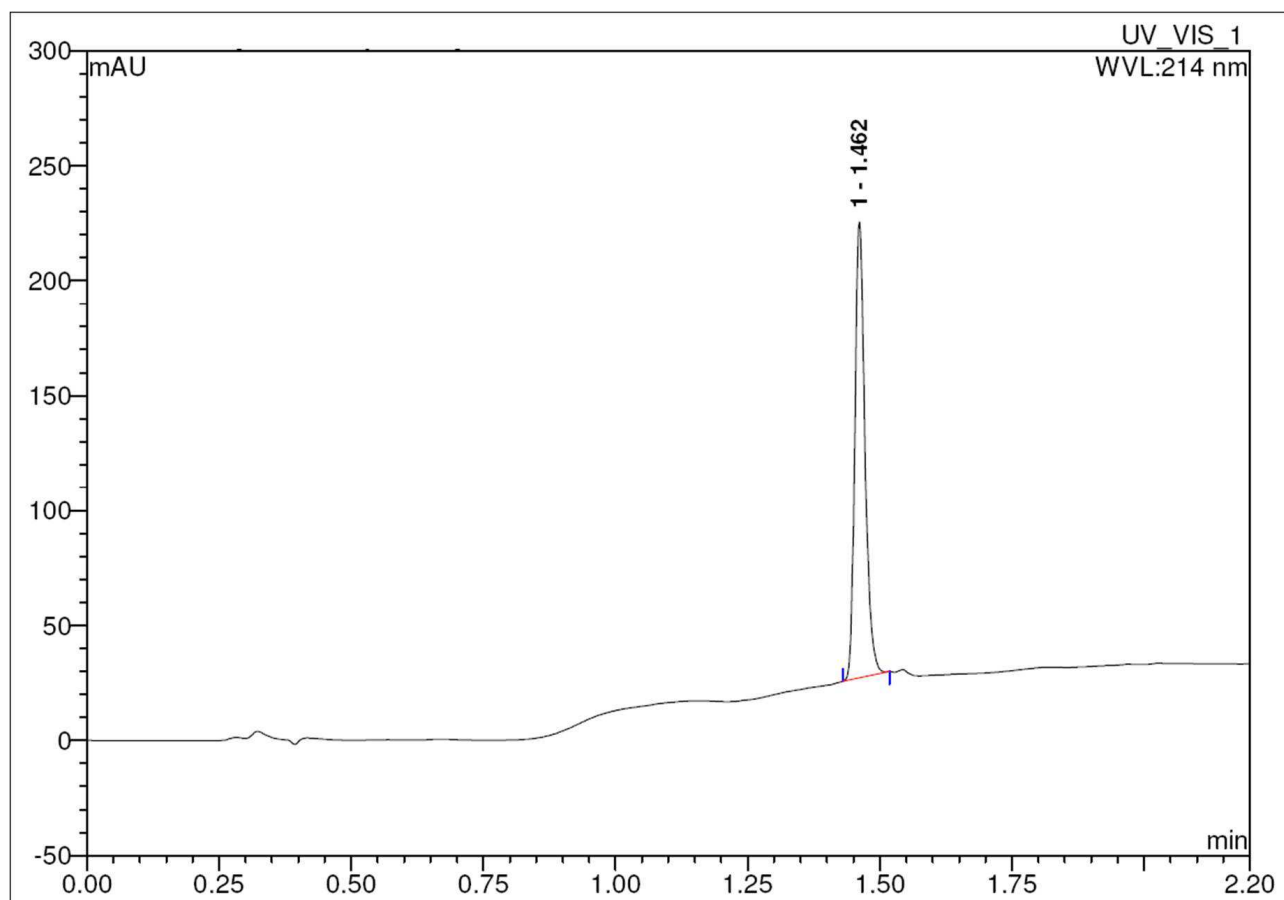


Figure S5. UPLC chromatogram of the purified bipyridine peptide dendrimer **BP1**. Conditions: 0-50 % B in 2.2 min, λ 214 nm.

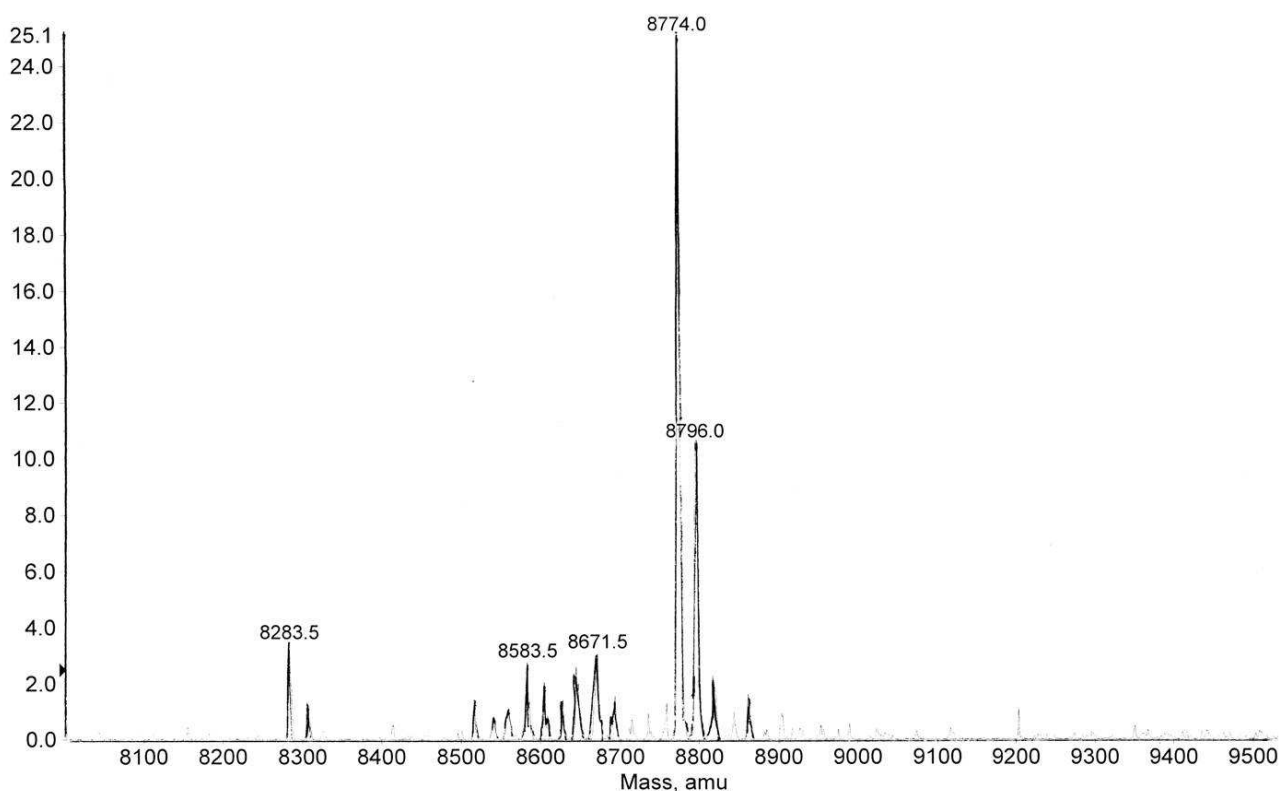


Figure S6. MS reconstruction for the purified bipyridine peptide dendrimer **BP1** (MALDI+). m/z 8774.0: $[M+H]^+$, clc 8775.5; m/z 8796.0: $[M+Na]^+$, clc 8797.5.

BP2

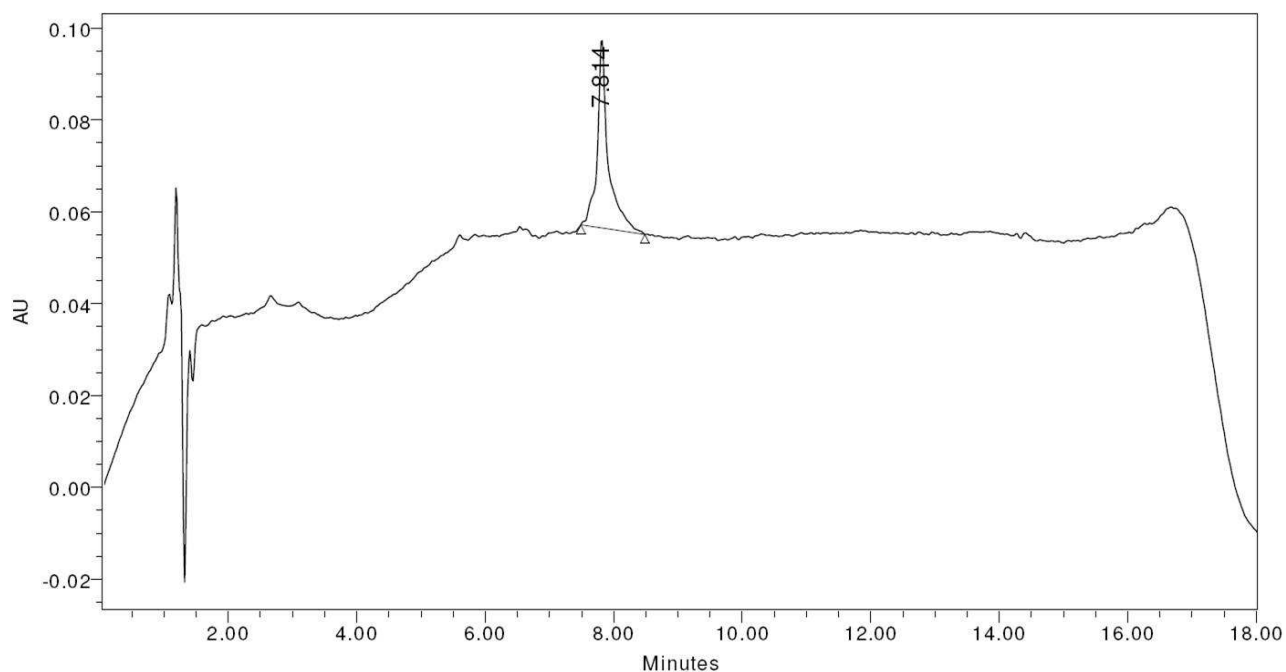


Figure S7. HPLC chromatogram of the purified bipyridine peptide dendrimer **BP2**. Conditions: 6-48 % B in 10 min, λ 214 nm.

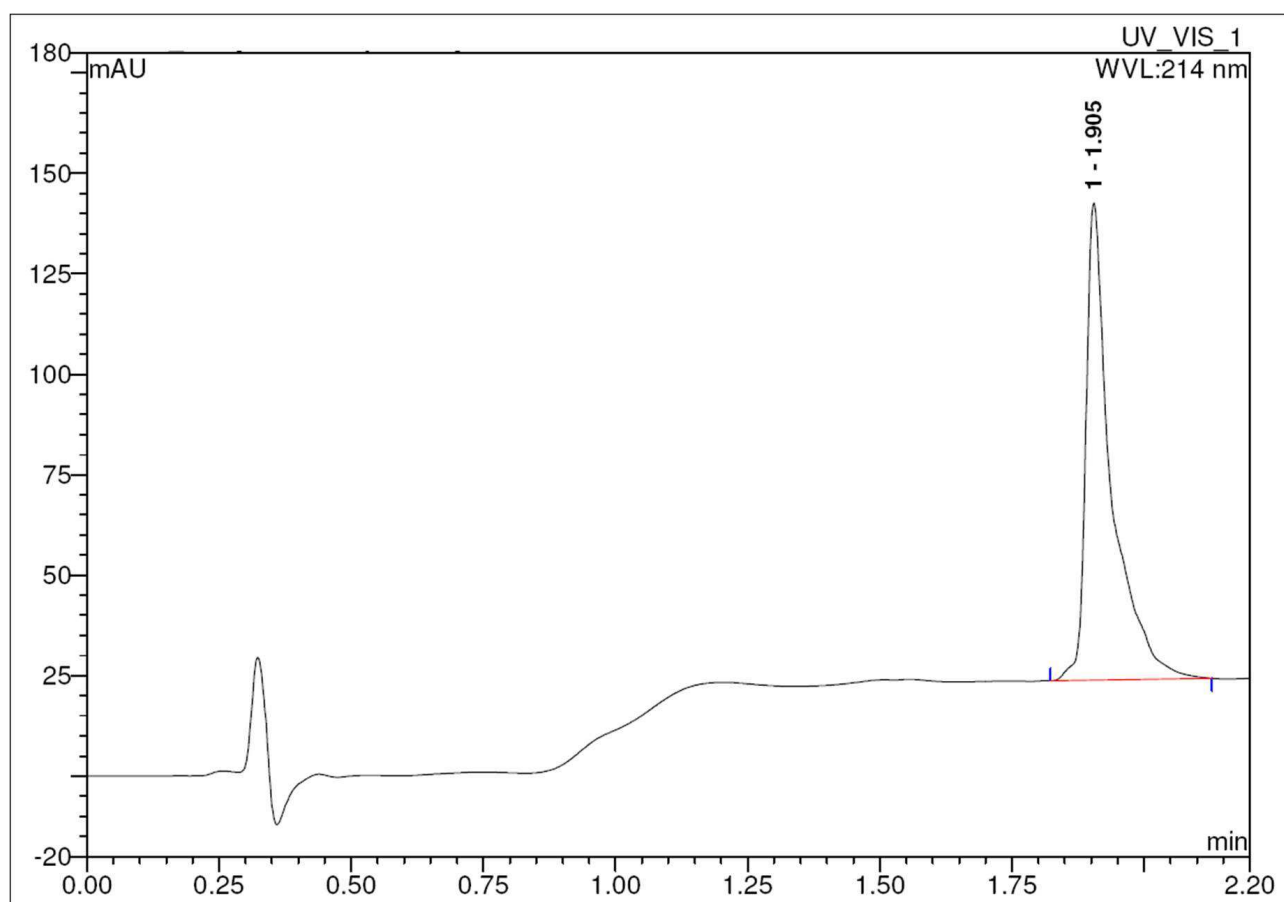


Figure S8. UPLC chromatogram of the purified bipyridine peptide dendrimer **BP2**. Conditions: 0-40 % B in 2.2 min, λ 214 nm.

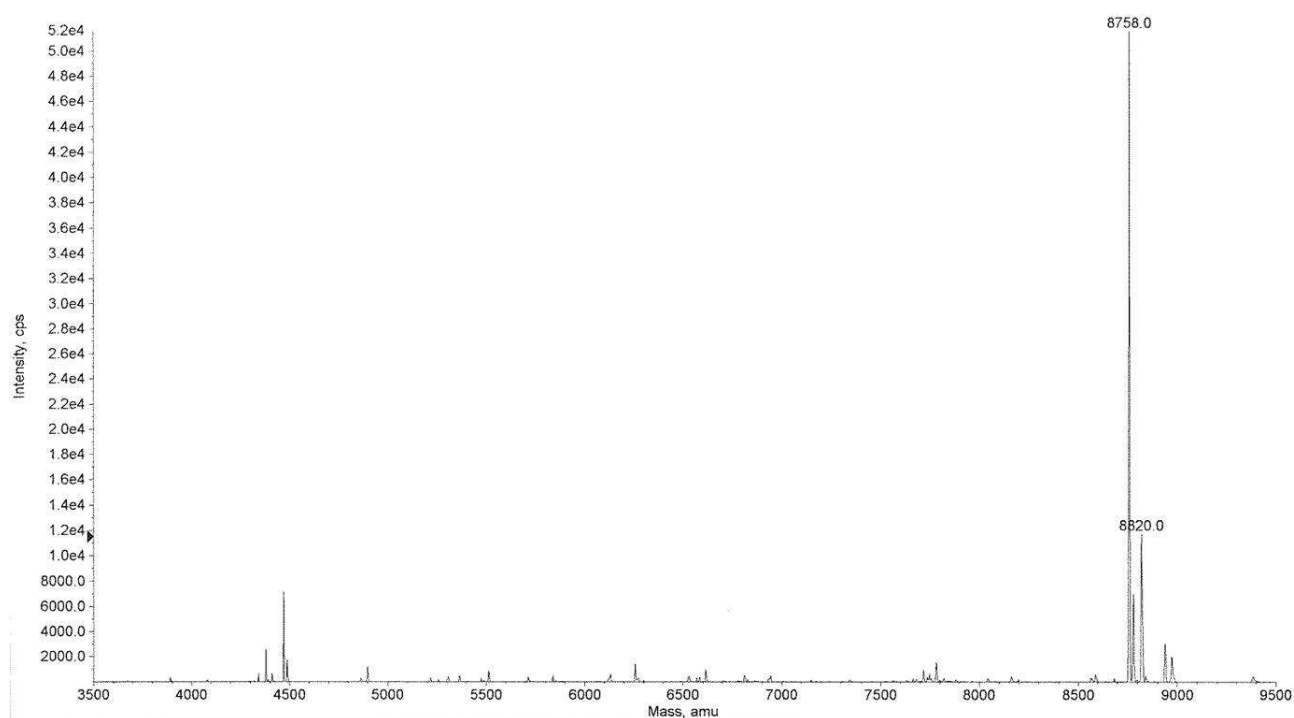


Figure S9. MS reconstruction for the purified bipyridine peptide dendrimer **BP2**. (ESI+ Q-Trap). m/z 8758.0: $[M+H]^+$, clc 8758.7; m/z 8820.0: $[M+K+Na-H]^+$, clc 8818.7.

BP3

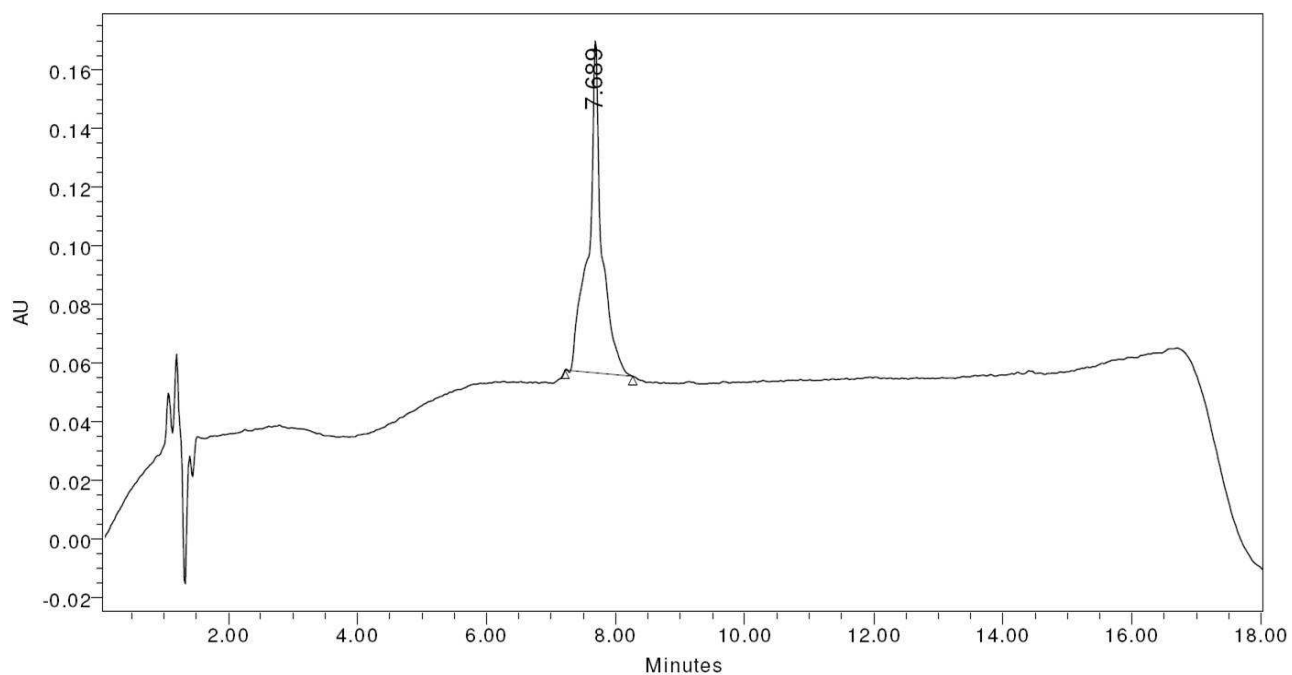


Figure S10. HPLC chromatogram of the purified bipyridine peptide dendrimer **BP3**. Conditions: 6-48 % B in 10 min, λ 214 nm.

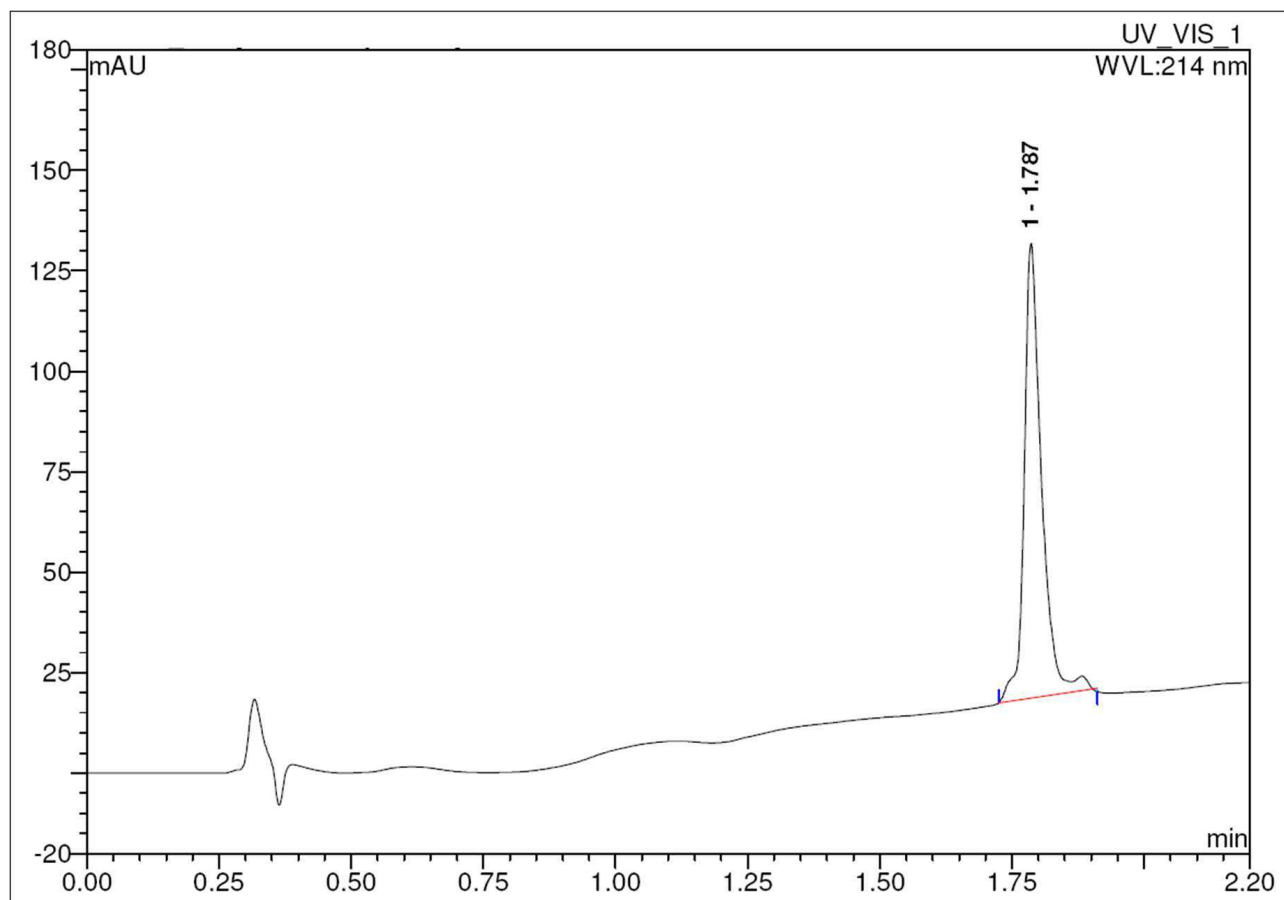


Figure S11. UPLC chromatogram of the purified bipyridine peptide dendrimer **BP3**. Conditions: 0-50 % B in 2.2 min, λ 214 nm.

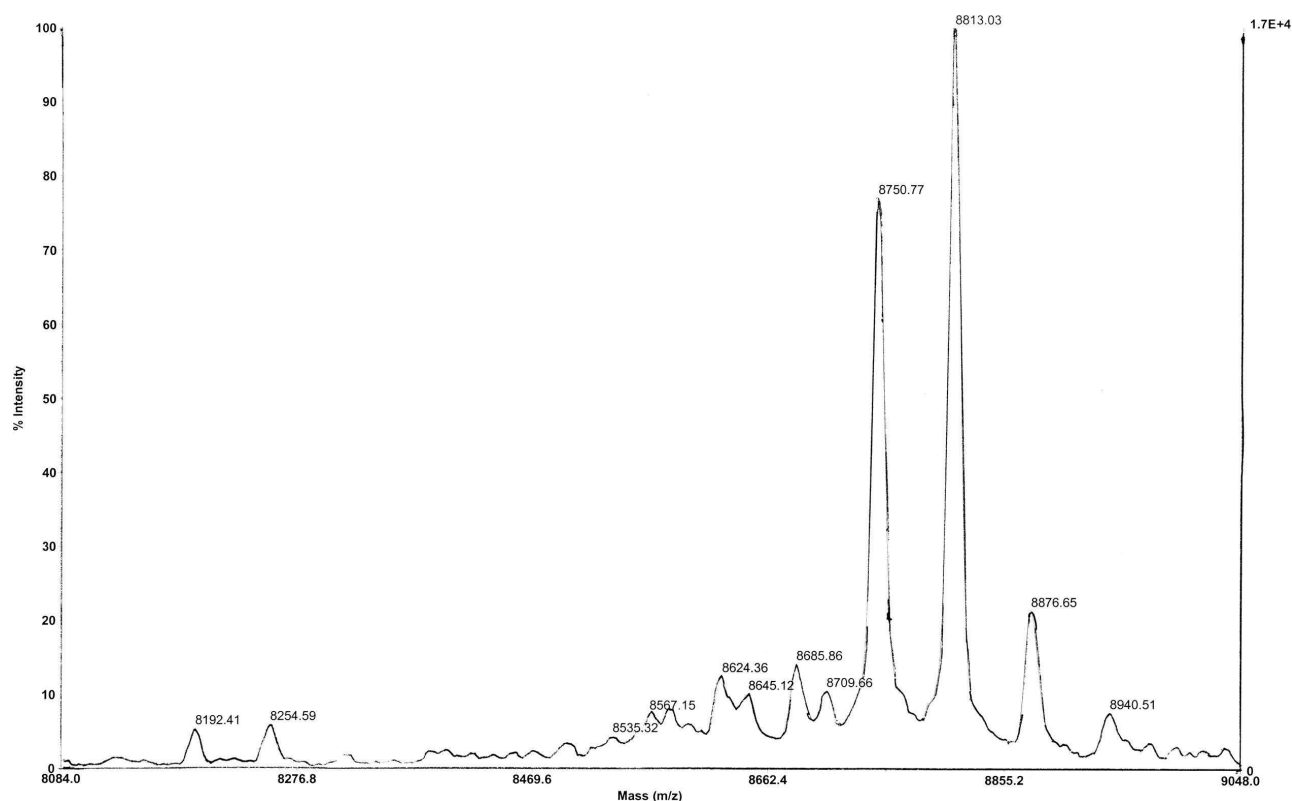


Figure S12. MS reconstruction for the purified bipyridine peptide dendrimer **BP3** (MALDI +). m/z 8750.77: $[M+H]^+$, clc 8751.9; m/z 8813.03: $[M+Na+K-H]^+$, clc 8812.9.

BP4

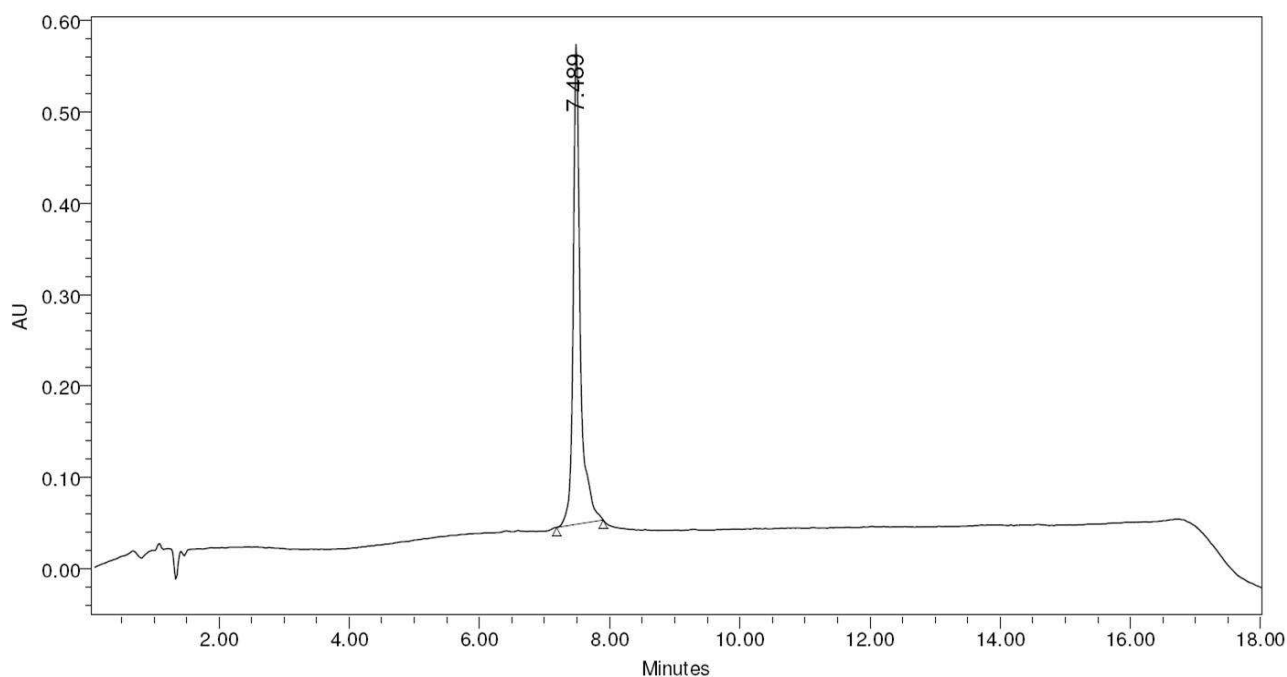


Figure S13. HPLC chromatogram of the purified bipyridine peptide dendrimer **BP4**. Conditions: 6-48 % B in 10 min, λ 214 nm.

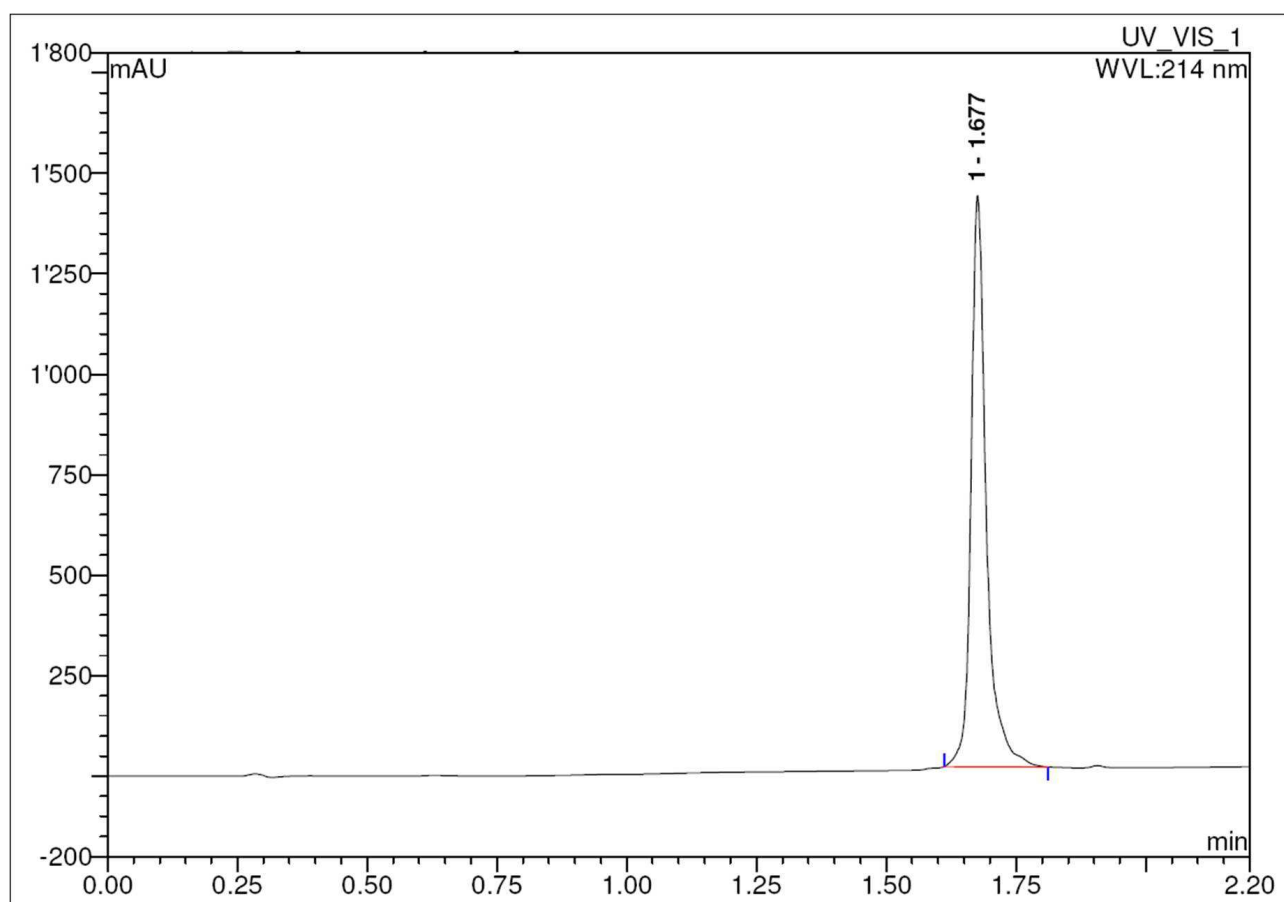


Figure S14. UPLC chromatogram of the purified bipyridine peptide dendrimer **BP4**. Conditions: 0-50 % B in 2.2 min, λ 214 nm.

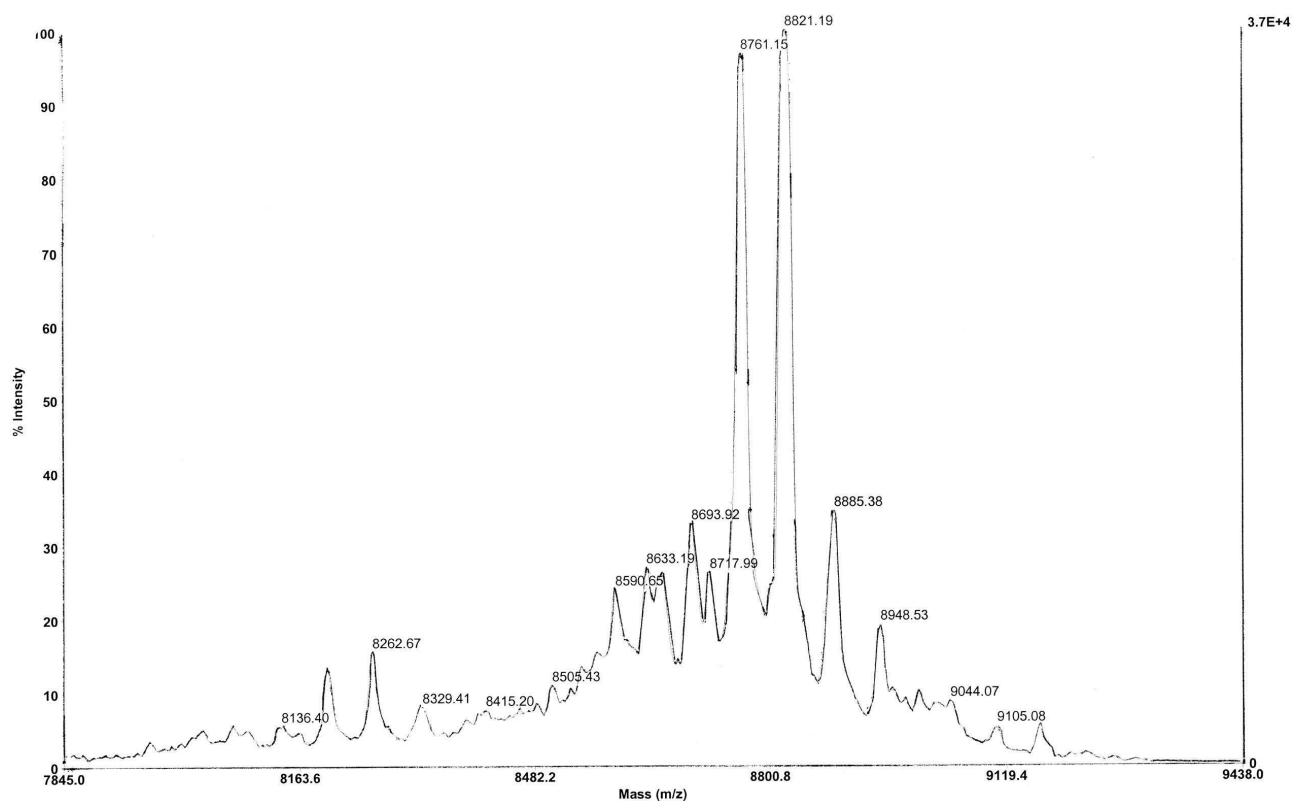


Figure S15. MS reconstruction for the purified bipyridine peptide dendrimer **BP4** (MALDI +). m/z 8761.15: $[M+H]^+$, clc 8759.4; m/z 8821.19: $[M+Na+K-H]^+$, clc 8819.5.

Metal binding tests

Data fitting procedure

The spectra were corrected for dilution after subtraction of the buffer contribution (obtained from blank spectra in the appropriate buffers). The presence of isosbestic points (ensuring that one predominant complex species was formed) was verified before starting the fitting procedure.

Titration curves were prepared using the absorbance at the wavelengths of the maxima of the start and end point of the titrations, as well as at the wavelength of maximum absorbance variation. Normalized titration curves were plotted using the ratio of the absorbance variation of each point ($\Delta A_{(i)}$) to the absorbance variation of the last point of the titration ($\Delta A_{(N)}$). The average of the normalized titration curves described above was taken as a measure of the molar fraction of the metal-bound dendrimer, x_{MDnd} , eq (1).

$$(1) \quad x_{MDnd(i)} = n_{MDnd(i)} / (n_{Dnd, tot}) = \Delta A_{(i)} / \Delta A_{\infty} \approx \Delta A_{(i)} / \Delta A_{(N)}$$

According to the mass action law (eq 2), for each experimental point (c_{Dnd} , c_M) the binding constant β_n can be obtained from the fraction of metal-bound dendrimer (x_{MDnd}). Conversely, given the binding constant, for each experimental point the fraction of metal-bound dendrimer can be exactly calculated by solving the $(n+1)^{th}$ grade equation derived by (2).

$$(2) \quad \beta_n = [MDnd] / ([M][Dnd]^n) = x_{MDnd} / ((c_M - c_{Dnd} \cdot x_{MDnd}) \cdot (c_{Dnd} \cdot (1 - x_{MDnd}))^{n-1})$$

The fitting algorithm calculated the binding constant which minimizes the least squared error on the experimental metal-bound dendrimer fraction. An iterative procedure was employed to compensate the error induced by non quantitative binding at the end of the titration experiment (that is for the difference between $\Delta A_{(N)}$ and ΔA_{∞} in (1)).

Fitting with different dendrimer concentrations confirmed the concentrations calculated from sample weight within ~15 % error.

Wherever uncertainties regarding binding stoichiometry could arise, fitting was performed for both theoretically possible binding stoichiometries and the two best fitting curves obtained were compared: in all cases one stoichiometry displayed a much better agreement with the experimental data.

Table S2. Variation of the Absorption Maxima of the Ligands upon Titration with Ni(II) and Fe(II)

ligand	metal	pH	$\lambda_{M,0}^a$ (nm)	$\lambda_{M,N}^b$ (nm)	λ_{MLCT}^c (nm)
BP1	Ni(II)	4.0	311	314 (+) ^d	
BP1	Ni(II)	6.5	297	312/319 ^e	
BP2	Ni(II)	4.0	312.5	313 (+) ^d	
BP2	Ni(II)	6.5	311.5	312.5 (+) ^d	
BP3	Ni(II)	4.0	309	313 (+) ^d	
BP3	Ni(II)	6.5	298	313	
BP4	Ni(II)	4.0	298	312.5/319.5 ^e	
BP4	Ni(II)	6.5	297	312.5	
BP1	Fe(II)	4.0	312	312 (+) ^d	534
BP1	Fe(II)	6.5	297	311	
BP2	Fe(II)	4.0	313	312.5 (+) ^d	532
BP2	Fe(II)	6.5	311	312.5 (+) ^d	
BP3	Fe(II)	4.0	308	312 (+) ^d	533.5
BP3	Fe(II)	6.5	298	311.5	532
BP4	Fe(II)	4.0	298	298 (-) ^f	
BP4	Fe(II)	6.5	302	309.5	
2:1 Mix ^g	Fe(II)	6.5	313	311 (+) ^d	532

^a Absorption maximum of the free ligand. ^b Final absorption maximum. ^c Maximum of the MLCT band, where present. ^d Increase in the band intensity (hyperchromicity) observed. ^e Two maxima observed. ^f Decrease in the band intensity (hypochromicity) observed. ^g 2:1 mixture of **BP4** and **BP1**.

Spectrophotometric titrations and titration curves fitting

Titration with Ni(II)

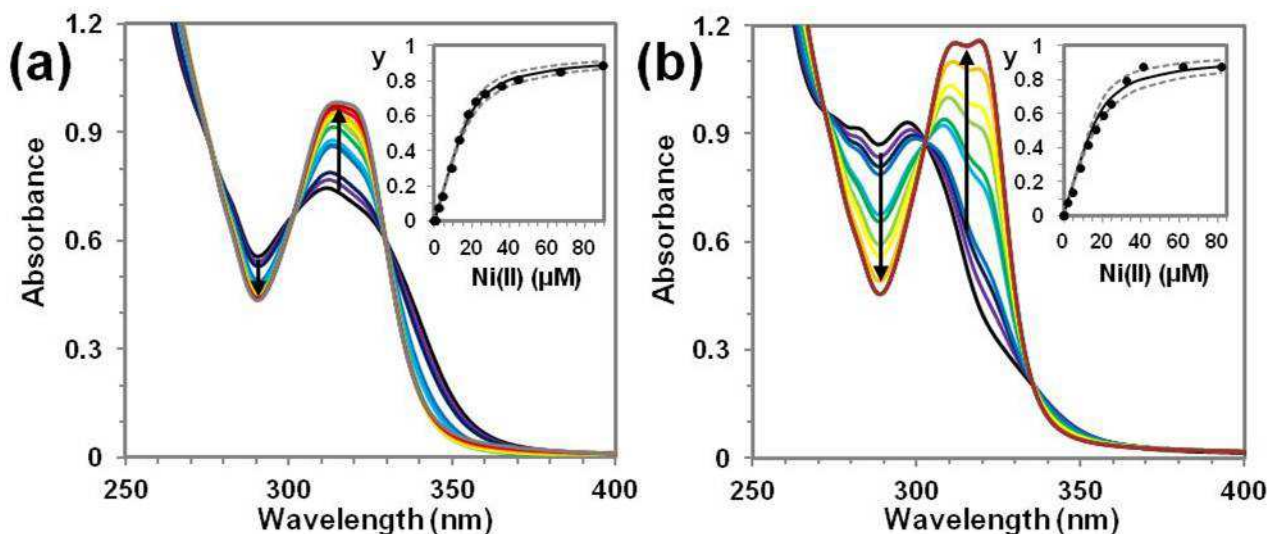


Figure S16. Spectrophotometric titrations of **BP1** with Ni(II) by addition of NiCl₂·6 H₂O: (a) 50 μM ligand in AcONa buffer, pH 4.0; (b) 50 μM ligand in HEPES buffer, pH 6.5. Insets with fitting of the normalized titration curves. y ($y = (A - A_0)/(A_\infty - A_0)$) is the fraction of metal bound ligand, the dotted lines represent the confidence interval for the calculated titration curve (solid line).

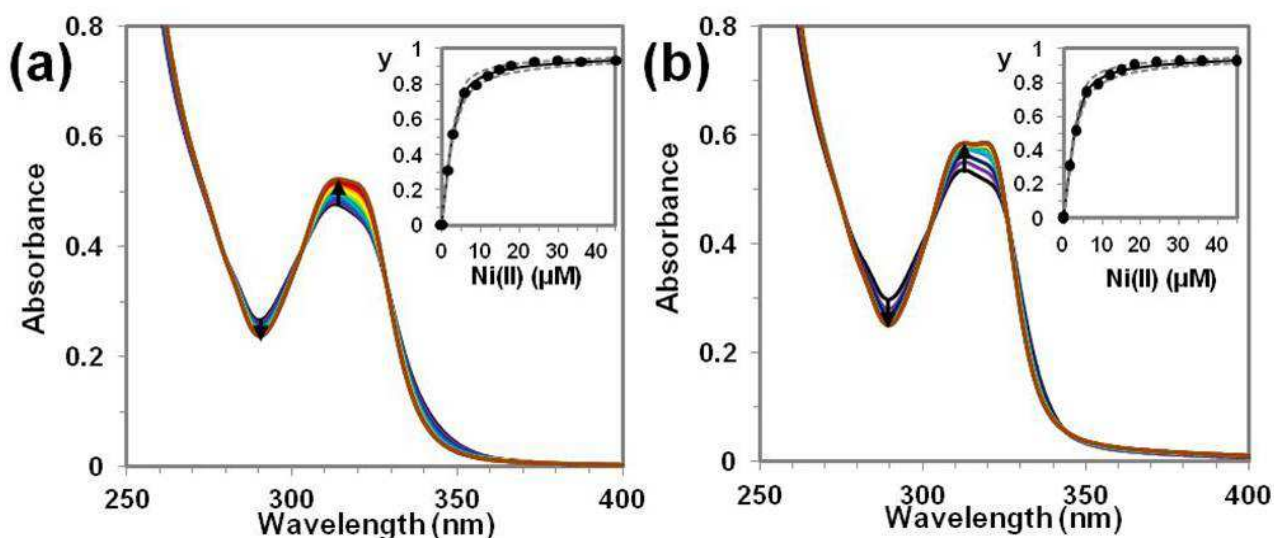


Figure S17. Spectrophotometric titrations of **BP2** with Ni(II) by addition of NiCl₂·6 H₂O: (a) 30 μM ligand in AcONa buffer, pH 4.0; (b) 30 μM ligand in HEPES buffer, pH 6.5. Insets with fitting of the normalized titration curves. y ($y = (A - A_0) / (A_{\infty} - A_0)$) is the fraction of metal bound ligand, the dotted lines represent the confidence interval for the calculated titration curve (solid line).

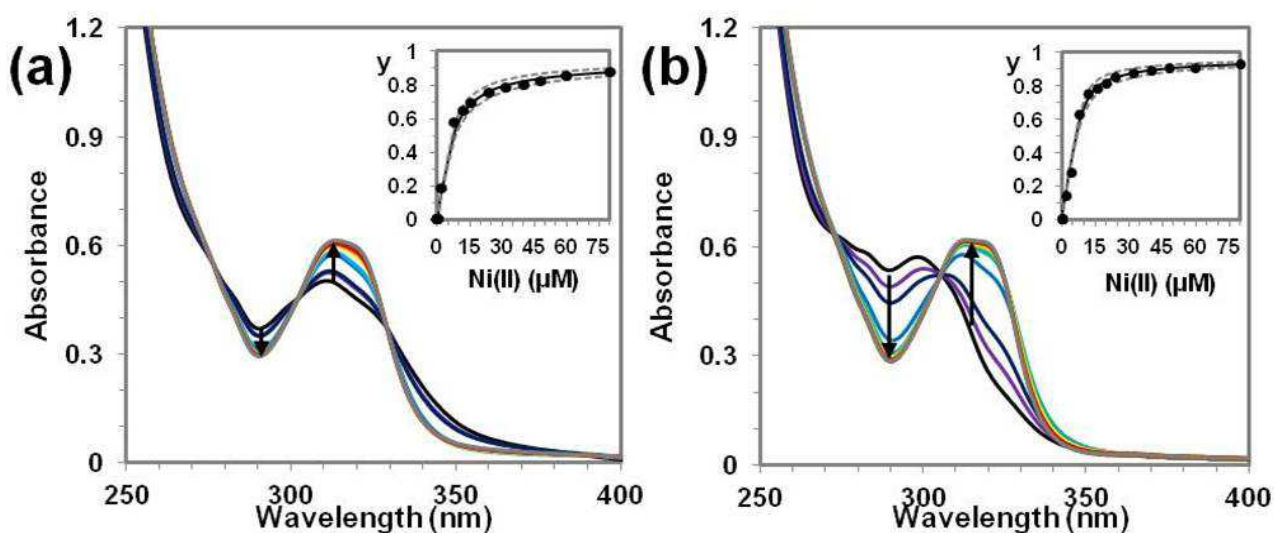


Figure S18. Spectrophotometric titrations of **BP3** with Ni(II) by addition of NiCl₂·6 H₂O: (a) 40 μM ligand in AcONa buffer, pH 4.0; (b) 40 μM ligand in HEPES buffer, pH 6.5. Insets with fitting of the normalized titration curves. y ($y = (A - A_0) / (A_{\infty} - A_0)$) is the fraction of metal bound ligand, the dotted lines represent the confidence interval for the calculated titration curve (solid line).

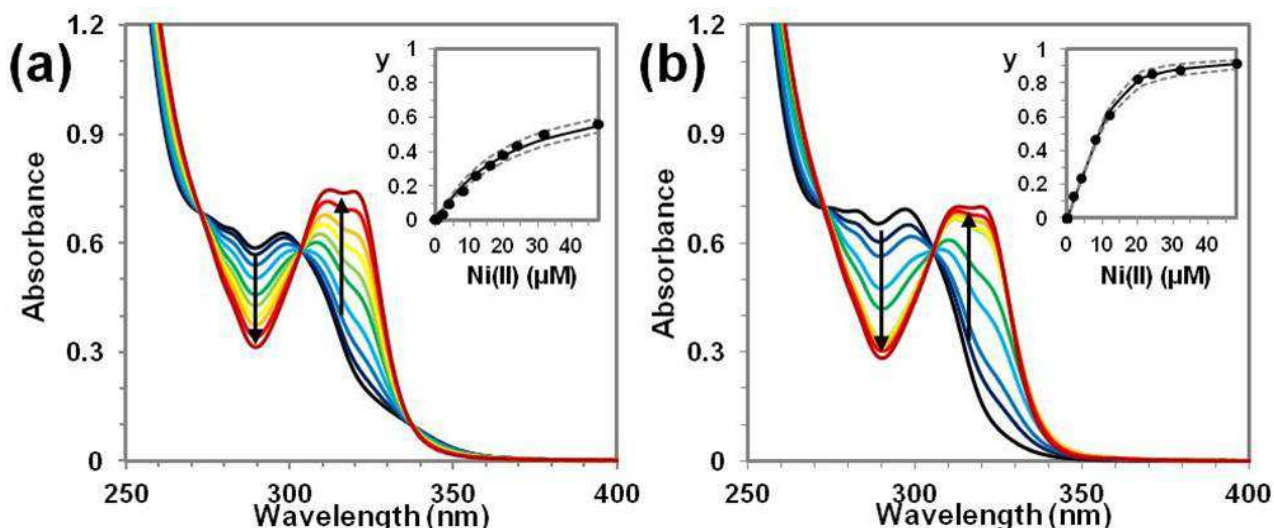


Figure S19. Spectrophotometric titrations of **BP4** with Ni(II) by addition of $\text{NiCl}_2 \cdot 6 \text{H}_2\text{O}$: (a) 40 μM ligand in AcONa buffer, pH 4.0; (b) 40 μM ligand in HEPES buffer, pH 6.5. Insets with fitting of the normalized titration curves. y ($y = (A - A_0) / (A_{\infty} - A_0)$) is the fraction of metal bound ligand, the dotted lines represent the confidence interval for the calculated titration curve (solid line).

Titration with Fe(II)

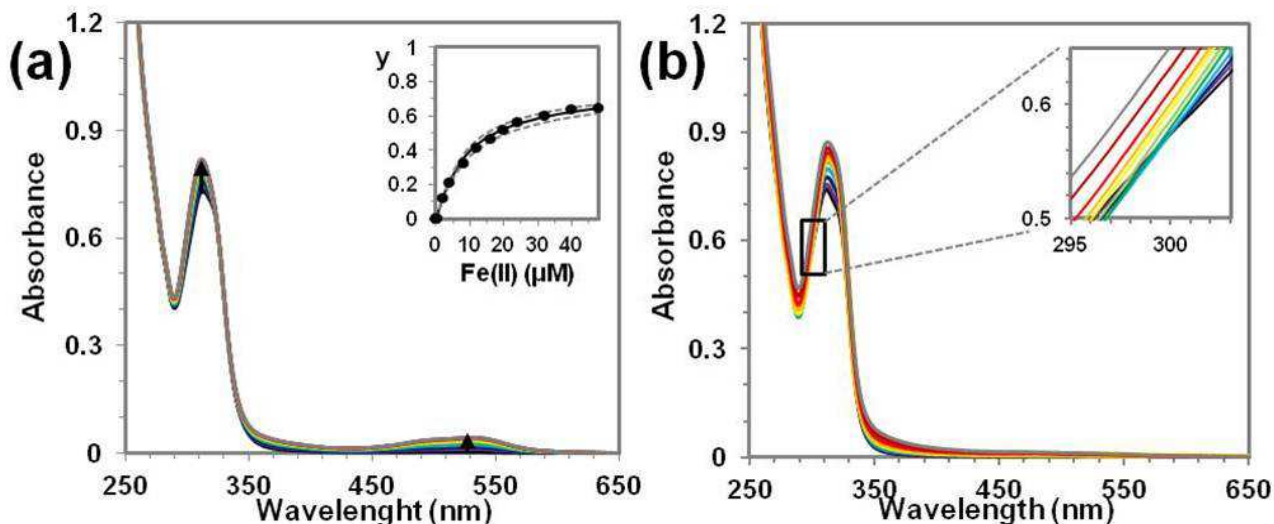


Figure S20. Spectrophotometric titrations of **BP2** with Fe(II) by addition of $\text{Fe}(\text{NH}_4)_2(\text{SO}_4)_2 \cdot 6 \text{H}_2\text{O}$: (a) 50 μM ligand in AcONa buffer, pH 4.0; (b) 50 μM ligand in HEPES buffer, pH 6.5. Inset in (a) with fitting of the normalized titration curve. y ($y = (A - A_0) / (A_{\infty} - A_0)$) is the fraction of metal bound ligand, the dotted lines represent the confidence interval for the calculated titration curve (solid line). Inset in (b) showing the loss of the isosbestic point at 299 nm when the concentration of added Fe(II) was higher than 15 μM .

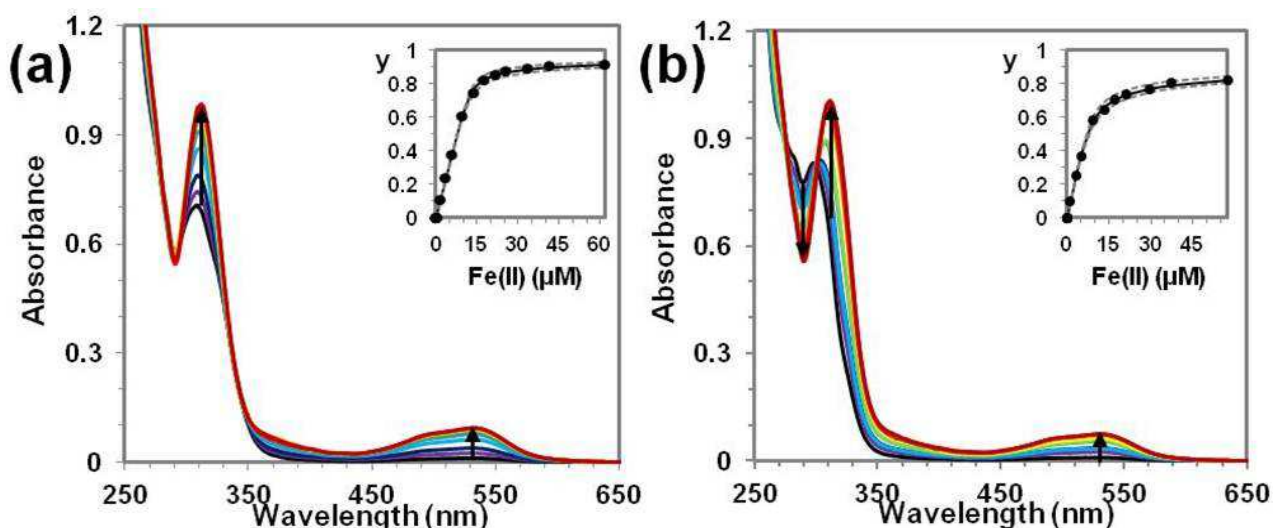


Figure S21. Spectrophotometric titrations of **BP3** with Fe(II) by addition of $\text{Fe}(\text{NH}_4)_2(\text{SO}_4)_2 \cdot 6 \text{H}_2\text{O}$: (a) 50 μM ligand in AcONa buffer, pH 4.0; (b) 50 μM ligand in HEPES buffer, pH 6.5. Insets with fitting of the normalized titration curves. y ($y = (A - A_0)/(A_\infty - A_0)$) is the fraction of metal bound ligand, the dotted lines represent the confidence interval for the calculated titration curve (solid line).

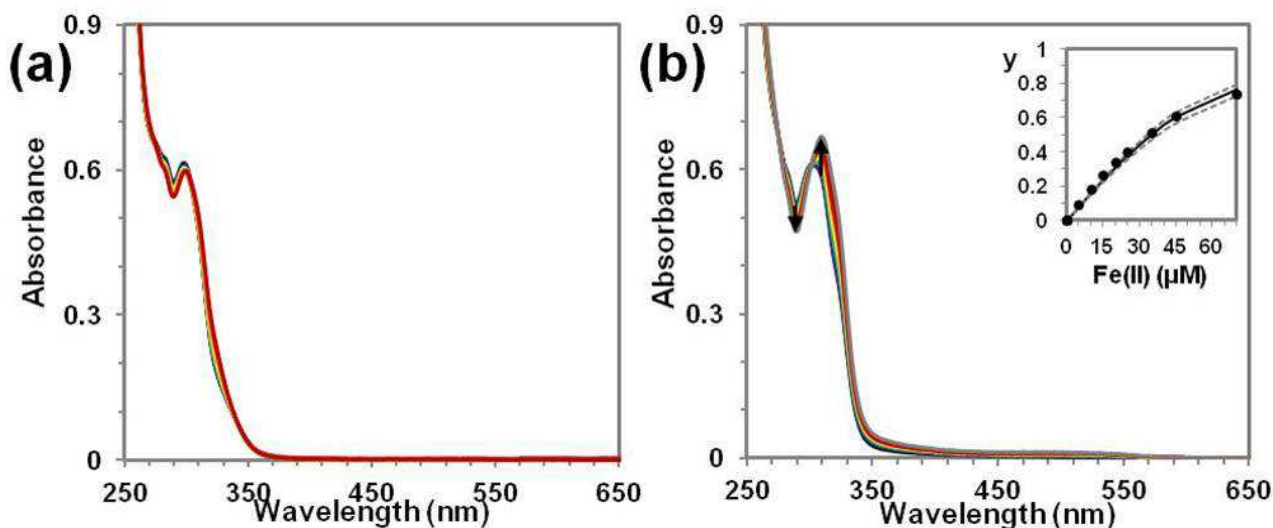


Figure S22. Spectrophotometric titrations of **BP4** with Fe(II) by addition of $\text{Fe}(\text{NH}_4)_2(\text{SO}_4)_2 \cdot 6 \text{H}_2\text{O}$: (a) 50 μM ligand in AcONa buffer, pH 4.0; (b) 50 μM ligand in HEPES buffer, pH 6.5. Inset in (b) with fitting of the normalized titration curve. y ($y = (A - A_0)/(A_\infty - A_0)$) is the fraction of metal bound ligand, the dotted lines represent the confidence interval for the calculated titration curve (solid line).

Characterization of the metal complexes

HPLC comparison of bipyridine dendrimer ligands and their metal complexes

Free ligand solutions prepared for the spectrophotometric titrations (30-50 μ M in AcONa buffer, pH 4.0, or in HEPES buffer, pH 6.5) were used as ligand standards, the final solutions obtained after the same experiments (containing 1.2-2.0 eq of Fe(II) or Ni(II), ligand dilution ≤ 4 %) were used as metal complex standards.

Solutions were diluted 1:1 with eluent A just before injection. Analytical chromatograms were recorded on the Waters 600 HPLC using the gradients 18-60 % B in 10 min or 6-48 % B in 10 min, monitoring at λ 214 nm and at λ 525 nm for Fe(II) complexes.

Table S3. Results of the HPLC Comparison of the Free Ligands and their Metal Complexes

ligand	t_r (min)	ligand	t_r ligand + Ni (II) (min)	t_r ligand + Fe(II), pH 4.0 ^a (min)	t_r ligand + Fe(II), pH 6.5 ^a (min)
BP1^b	5.18		5.12	5.15	5.39
BP2^c	7.81		7.78	20 % 7.73, 80 % 7.90	7.82
BP3^c	7.69		7.68	7.58	7.80
BP4^c	7.49		ND ^d	ND ^d	15 % 7.39, 85 % 7.49

^a Peaks detected also at λ 525 nm are bold. ^b The gradient 18-60 % B in 10 min was used for the analyses.

^c The gradient 6-48 % B in 10 min was used for the analyses. ^d No data.

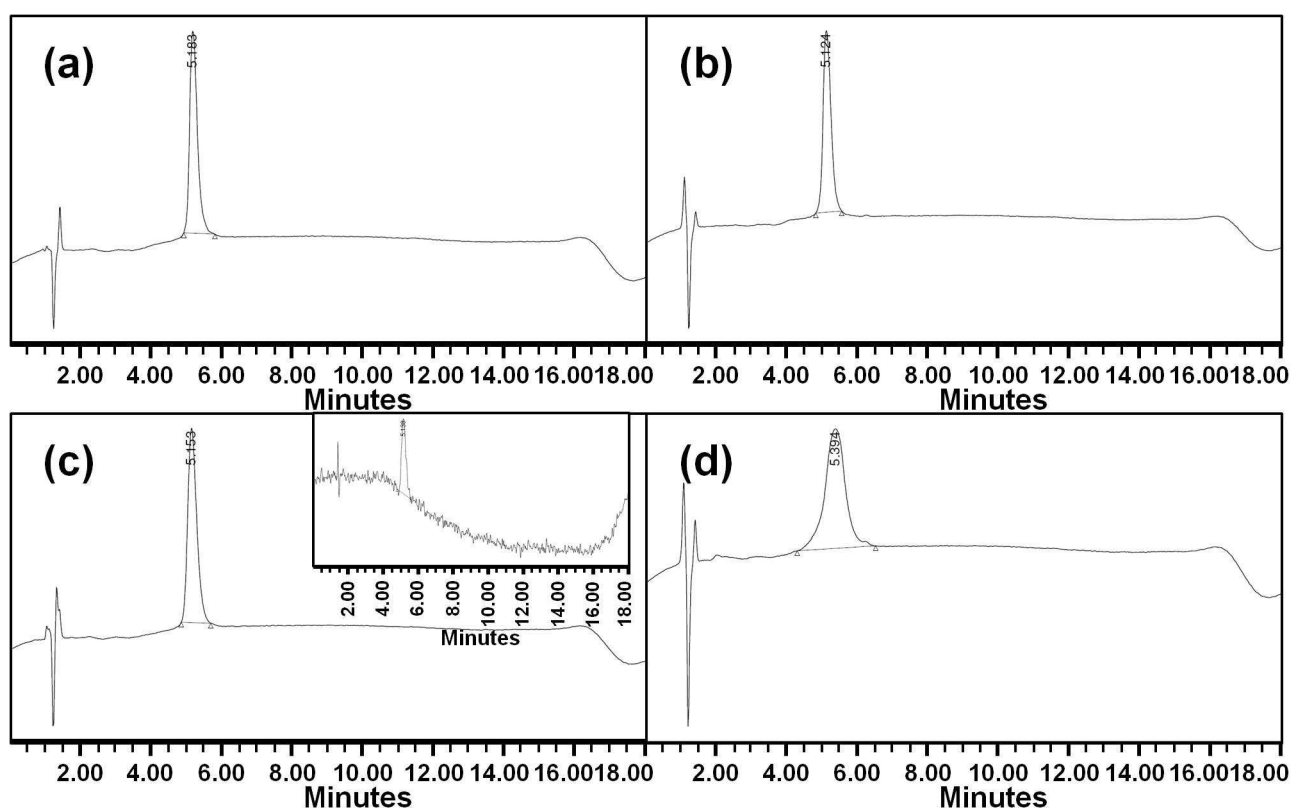


Figure S23. HPLC comparison of the ligand **BP1** (a), of its Ni(II) complex (b), and of its Fe(II) complexes in AcONa buffer, pH 4.0 (c) and in HEPES buffer, pH 6.5 (d). Conditions: 50 μ M ligand, 1.5 eq metal, analysis on the Waters 600 HPLC, 18-60 % B in 10 min, detection at λ 214 nm (inset in (c) detected at λ 525 nm, selective for [Fe^{II}(bipy)₃]-like complexes).

Spectrophotometric test of reversibility of the stoichiometric change in Fe(II) complex formation for BP1

The peptide dendrimer **BP1** was dissolved in 12 mM AcOH under argon to a concentration of 50 μ M and 1.0 mL of the resulting solution was transferred in a septum stoppered UV cell. After recording the spectrum of the free ligand, 25 μ L 2.5 mM $\text{Fe}(\text{NH}_4)_2(\text{SO}_4)_2$ (1.2 eq) were added and the spectrum was recorded after 1 and 2 h. The pH was brought to 6.5 by addition of 16 μ L 1.0 M NaOH and spectra were recorded after 1, 2, 4, 8 h. The pH was brought to 4.0 by addition of 12 μ L 1.0 M HCl and spectra were recorded after 12, 24 h. The pH was brought back to 6.5 by addition of 12 μ L 1.0 M of NaOH and a spectrum was recorded after 24 h. Finally, the pH was brought back to 4.0 by addition of 12 μ L 1.0 M HCl and a spectrum was recorded after 12 h.

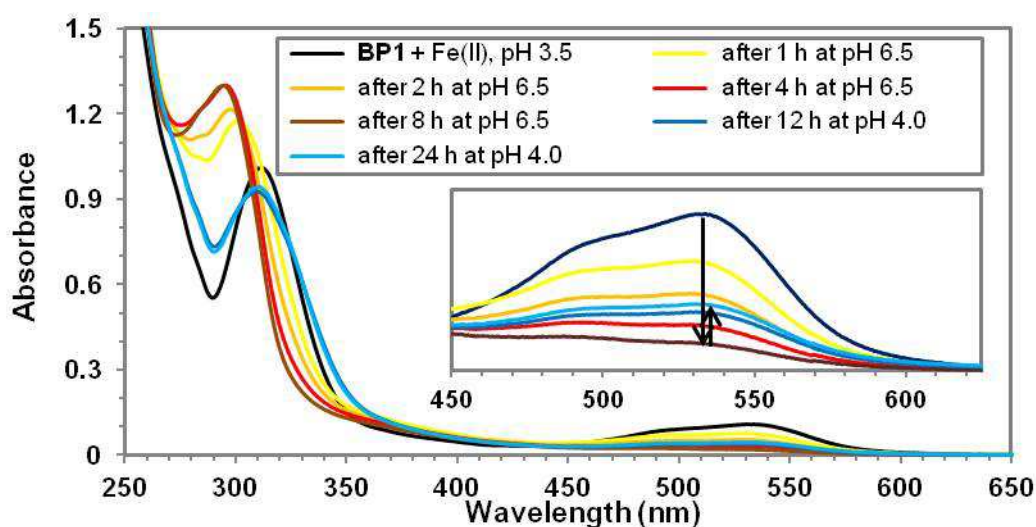


Figure S24. Spectrophotometric test of the change in Fe(II) binding stoichiometry upon pH change for the bipyridine dendrimer ligand **BP1**. The ligand, 50 μ M in AcOH 12 mM, is added with 1.2 eq Fe(II). After equilibration, the pH is shifted to 6.5 by addition of 1 M NaOH and spectra are acquired at increasing times until disappearance of the MLCT band (inset), then the pH is brought back to 4.0 by addition of 1 M HCl and spectra are acquired until no further increase in the intensity of the MLCT band is observed. Times given are referred to the last pH switch. The incomplete recovery is probably due to partial oxidation of Fe(II) at pH 6.5 by atmospheric oxygen leaking into the cell.

Determination of the apparent pK_a

The lyophilized bipyridine peptide dendrimer **BP1** was dissolved in milliQ H_2O to a concentration of 0.20 mM. 0.25 mL aliquots of the resulting solution were added with 40 μ L HCl 4 mM (3.2 eq). For measurements on the 3:1 Fe(II) complex of **BP1**, 0.50 eq of a 5.0 mM solution of $Fe(NH_4)_2(SO_4)_2 \cdot 6 H_2O$ (freshly prepared under argon) were added to the acidified ligand solution and the mixture was allowed to equilibrate with exclusion of air until the characteristic 3:1 Fe(II) complex color was observed.

The initial pH of the sample was read, then aliquots of 5 μ L NaOH 5.0 mM (0.5 eq) were added and after equilibration the pH was read. NaOH additions continued until $pH \geq 9$. For each experiment a graph of the buffering power ($\Delta V_{NaOH}/\Delta pH$) was built and the apparent pK_a was obtained from the maximum of the smoothed graph.

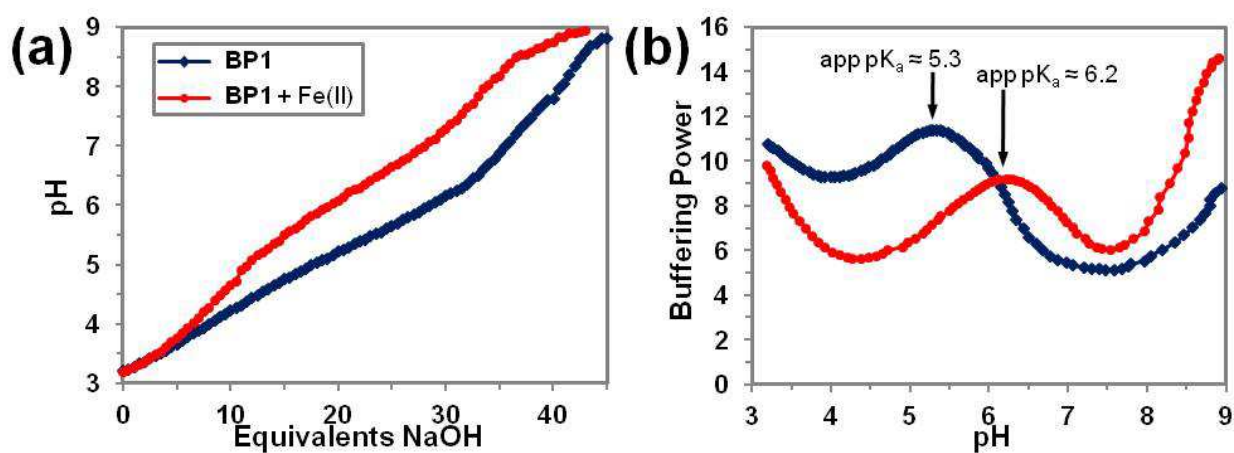


Figure S25. (a) Acid-base titration of the free bipyridine dendrimer ligand **BP1** and of the same ligand in the presence of 0.5 eq Fe(II). (b) Calculated buffering power (equivalents of base for unit pH variation) for the free ligand and for the ligand in the presence of 0.5 eq Fe(II). Conditions: initial ligand concentration 0.2 mM in H_2O plus 3.2 eq 4 mM HCl, addition of 0.5 eq 5 mM NaOH per point. The peak in the buffering power graph shows the apparent pK_a of the 26 side-chain carboxylic groups of the peptide dendrimer.

BP1/BP4 mixed Fe(II) complex

Job-plot analysis of Fe(II) complexation by BP1/BP4 mixtures

The bipyridine dendrimer ligands **BP1** and **BP4** were dissolved in 20 mM HEPES buffer, pH 6.5, at 0.20 mM concentration. Mixtures of the two solutions containing $n \cdot 5 \mu\text{L}$ ($n = 0-10$) of the former and $5 \cdot (10-n) \mu\text{L}$ of the latter (total dendrimer ligand amount: 10 nmol) were transferred into 11 wells of a microtiter plate and diluted with 100 μL HEPES buffer (total dendrimer ligand concentration 67 μM). A control well was filled with 150 μL HEPES buffer. The plate was read in the interval $280 \leq \lambda/\text{nm} \leq 600$, $\Delta\lambda = 3 \text{ nm}$. 3 μL 5.0 mM $\text{Fe}(\text{NH}_4)_2(\text{SO}_4)_2$ (15 nmol) were added to each well and after 1 h equilibration the plate was read again. The control spectrum was subtracted from the sample spectra and a Job plot (Figure S26) was prepared by plotting the absorbance increase at λ 525 nm (around the expected maximum of the MLCT band for $[\text{Fe}^{\text{II}}(\text{bipy})_3]$ -like complexes) against the molar fraction of dendrimer ligand **BP1** (x_{BP1}).

The maximum of the Job-plot lied in the interval $0.3 < x_{\text{BP1}} < 0.4$, thus supporting a 2:1 **BP4/BP1** ligand ratio, in agreement with the complex formula $[\text{Fe}^{\text{II}}(\text{BP4})_2(\text{BP1})]$, corresponding to the 3:1 Fe(II) complex with the lowest net charge at pH 6.5 (Table S4).

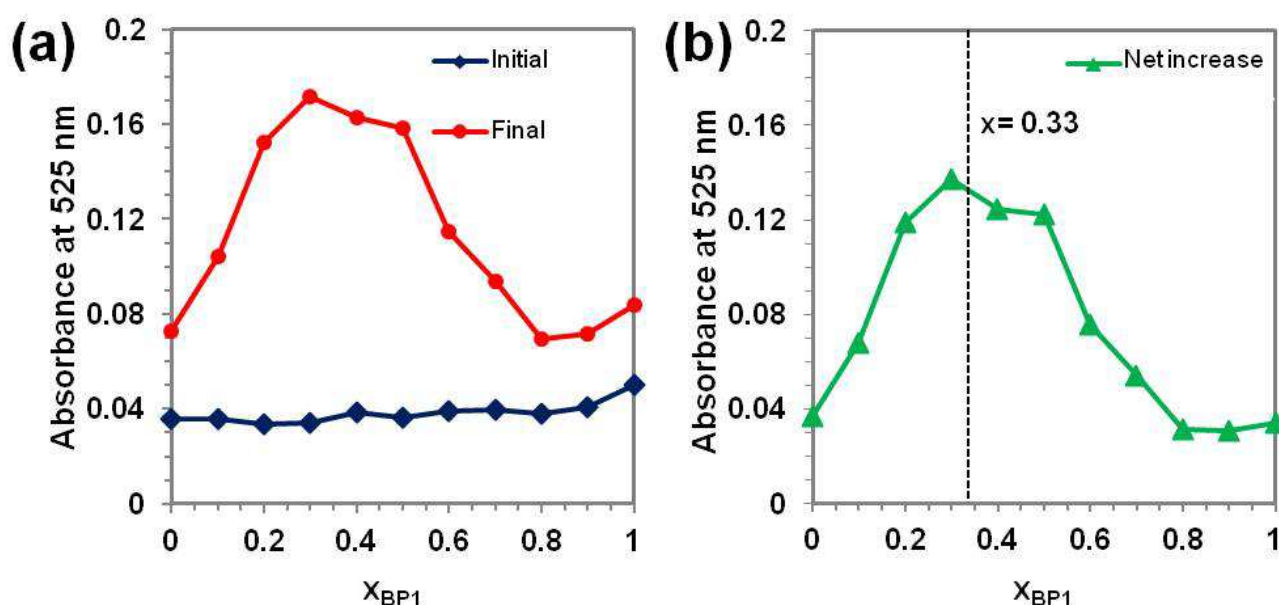


Figure S26. Job-plot experiment on mixtures of **BP1** and **BP4** added with 1.5 eq Fe(II): absorbance variation at λ 525 nm (a) and net absorbance increase (b) against molar fraction of **BP1** (x_{BP1}). The dashed line in (b) represents the molar fraction corresponding to the composition of the mixed complex $[\text{Fe}(\text{BP4})_2(\text{BP1})]$. Conditions: total dendrimer ligand concentration 67 μM in 20 mM HEPES buffer, pH 6.5.

Table S4. Total Net Charge of Triplets of **BP4** and **BP1** at Acidic and Neutral pH

ratio BP4/BP1	total net charge pH 4.0 ^a		total net charge pH 6.5 ^a	
	3 ligands	3:1 Fe(II) complex ^b	3 ligands	3:1 Fe(II) complex ^b
0 : 3	0	+ 2	- 78	- 76
1 : 2	+ 16	+ 18 ^c	- 46	- 44
2 : 1	+ 32	+ 34	- 14	- 12
3 : 0	+ 48	+ 50	+ 18	+ 20

^a Total net charges at pH 4.0 and 6.5 are calculated considering the side-chain carboxylic functions fully protonated or deprotonated, respectively, whereas the side-chain amino groups are assumed to be always fully protonated. ^b Actually observed 3:1 Fe(II) complexes are marked in bold. ^c This complex was most likely detected by HPLC in a mixture (see Table S5), but never found as only species formed.

Characterization of the complex $[\text{Fe}^{\text{II}}(\text{BP4})_2(\text{BP1})]$

HPLC

Solutions of the pure ligands, of each of the ligands plus 1.5 eq Fe(II) and a 2:1 mixture of the ligands, all at a (total) concentration of 50 μM in HEPES buffer, pH 6.5, as well as the content of the well which displayed the strongest MLCT band ($x_{\text{N1}} = 0.3$) in the Job plot experiment, were diluted 1:1 with eluent A. A 2:1 mixture of the ligands at a total concentration of 50 μM in AcONa buffer, pH 4.0, plus 1.5 eq Fe(II) was also tested. Analytical chromatograms were recorded on the Waters 600 HPLC using the gradient 6-48 % B in 10 min, monitoring at λ 214 and 525 nm

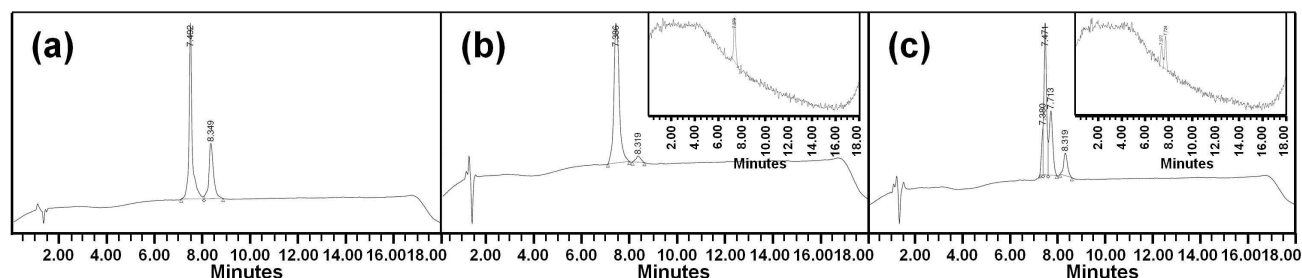


Figure S27. HPLC chromatograms of **BP4/BP1** 2:1 mixtures, total concentration about 65 μM . (a) Mixture in HEPES buffer, pH 6.5, in the absence of Fe(II). (b) Mixture in HEPES buffer, pH 6.5, added with 1.5 eq Fe(II). (c) Mixture in AcONa buffer, pH 4.0, added with 1.5 eq Fe(II). Insets in (b) and (c): chromatograms detected at $\lambda = 525$ nm (selective for $[\text{Fe}^{\text{II}}(\text{bipy})_3]$ -like complexes).

Table S5. HPLC Comparison of the Dendrimer Ligands **BP4** and **BP1** and of their Mixed Fe(II) Complexes at pH 6.5 and 4.0

	BP1	BP4	2:1 Mix ^a	2:1 Mix + 1.5 eq Fe(II), pH 6.5 ^b	2:1 Mix + 1.5 eq Fe(II), pH 4.0 ^c
λ 214 nm	8.35 min	7.49 min	67.7 % 7.49 min, 32.3 % 8.35 min	96.1 % 7.39 min, 3.9 % 8.32 min	8.3 % 7.38 min, 50.7 % 7.47 min, 29.7 % 7.71 min, ^d 11.3 % 8.32 min
λ 525 nm	-	-	-	7.38 min	40.2 % 7.38 min, 59.8 % 7.72 min ^d

^a 2:1 mixture of **BP4** and **BP1**, total concentration 50 μM , in HEPES buffer, pH 6.5. ^b 2:1 mixture of **BP4** and **BP1**, total concentration 65 μM , in HEPES buffer, pH 6.5, plus 1.5 eq $\text{Fe}(\text{NH}_4)_2(\text{SO}_4)_2$. ^c 2:1 mixture of **BP4** and **BP1**, total concentration 50 μM , in AcONa buffer, pH 4.0, plus 1.5 eq $\text{Fe}(\text{NH}_4)_2(\text{SO}_4)_2$. ^d The peak at tr 7.71 min can be identified as $[\text{Fe}(\text{BP4})(\text{BP1})_2]$, since it is a $[\text{Fe}^{\text{II}}(\text{bipy})_3]$ -like complex (active at λ 525 nm) and its stoichiometry balances the repartition of both ligands at λ 214 nm, see Table S6.

Table S6 Stoichiometric Balance of the Ligand Composition for 2:1 Mix + 1.5 eq Fe(II), pH 4.0 (Last Column in Table S5)

Composition	Found ^a	Attribution	BP1	BP4
33.3 % BP1 , 66.7 % BP4	8.3 % 7.38 min , 50.7 % 7.47 min, 29.7 % 7.71 min , 11.3 % 8.32 min	$[\text{Fe}(\text{BP4})_2(\text{BP1})]$ BP4 $[\text{Fe}(\text{BP4})(\text{BP1})_2]$ BP1	8.3 % · 1/3 + 29.7 % · 2/3 + 11.3 % = 33.9 %	8.3 % · 2/3 + 50.7 % + 29.7 % · 1/3 + = 66.1 %

^a Relative area at λ 214 nm; peaks detected also at λ 525 nm are marked bold.

At pH 6.5 only one 3:1 Fe(II) mixed complex is formed (see also Figure S27), with the formula $[\text{Fe}(\text{BP4})_2(\text{BP1})]$, as obtained by the Job-plot experiment. This complex has the smallest predicted net charge under the experimental conditions (see Table S4). At pH 4.0 two 3:1 mixed Fe(II) complexes are observed and a different complex, identified with $[\text{Fe}(\text{BP4})(\text{BP1})_2]$, prevails. This is most likely due to the fact that at pH 4.0 the latter complex has a smaller net positive charge than the former (see Table S4).

UV-Vis

A 2:1 mixture of **BP4** and **BP1** at a total concentration of 50 μM in HEPES buffer, pH 6.5, was prepared by dilution of solutions of the pure ligands in milliQ H_2O . 1.00 mL of this solution was titrated with 2.5 mM $\text{Fe}(\text{NH}_4)_2(\text{SO}_4)_2$ as described in the main text for the single ligands and the acquired spectra were treated as described above (Figure S28).

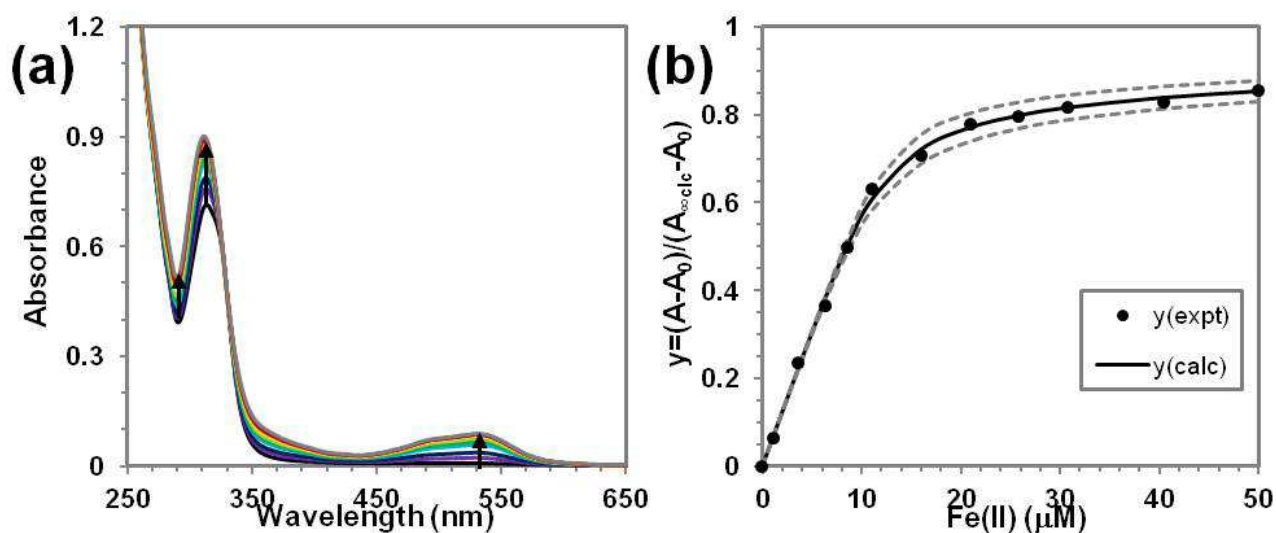


Figure S28. (a) Spectrophotometric titration of a 2:1 mixture of **BP4** and **BP1**, total concentration 50 μM in HEPES buffer, pH 6.5, by addition of 2.5 mM $\text{Fe}(\text{NH}_4)_2(\text{SO}_4)_2$. (b) Fitting of the normalized titration curve (relative absorbance variation, y , against amount of metal added) for the same experiment assuming the formation of the complex $[\text{Fe}(\text{BP4})_2(\text{BP1})]$. The gray dashed lines represent the confidence interval for the calculated titration curve.

NMR diffusion measurements

The lyophilized bipyridine peptide dendrimers were dissolved in 0.5-0.6 mL D₂O to a concentration of 0.3-1.0 mM and their pH was adjusted to the target value (4.0 or 6.5) by addition of 0.2 M NaOD (freshly prepared by careful addition of ice cold D₂O to NaH). 3:1 Fe(II) complex solutions were prepared by addition of 0.28-0.32 eq of a 10-15 mM solution of Fe(NH₄)₂(SO₄)₂·6H₂O in D₂O (freshly prepared under argon).

The probes for the 2:1 **BP4/BP1** mixture and its Fe(II) complex were prepared as follows: the lyophilized peptide dendrimers were dissolved in D₂O at a concentration of 0.5 mM for **BP1** and 1.0 mM for **BP4**. In two Eppendorf vials 0.25 mL of each solution were mixed and the pH of the resulting solutions was adjusted to 6.5-7 with 0.2 M NaOD, then 10 µL 11 mM Fe(NH₄)₂(SO₄)₂ in D₂O (0.88 eq) were added to one solution.

All samples were transferred into NMR tubes which were closed and protected from humidity and air with ParafilmTM.

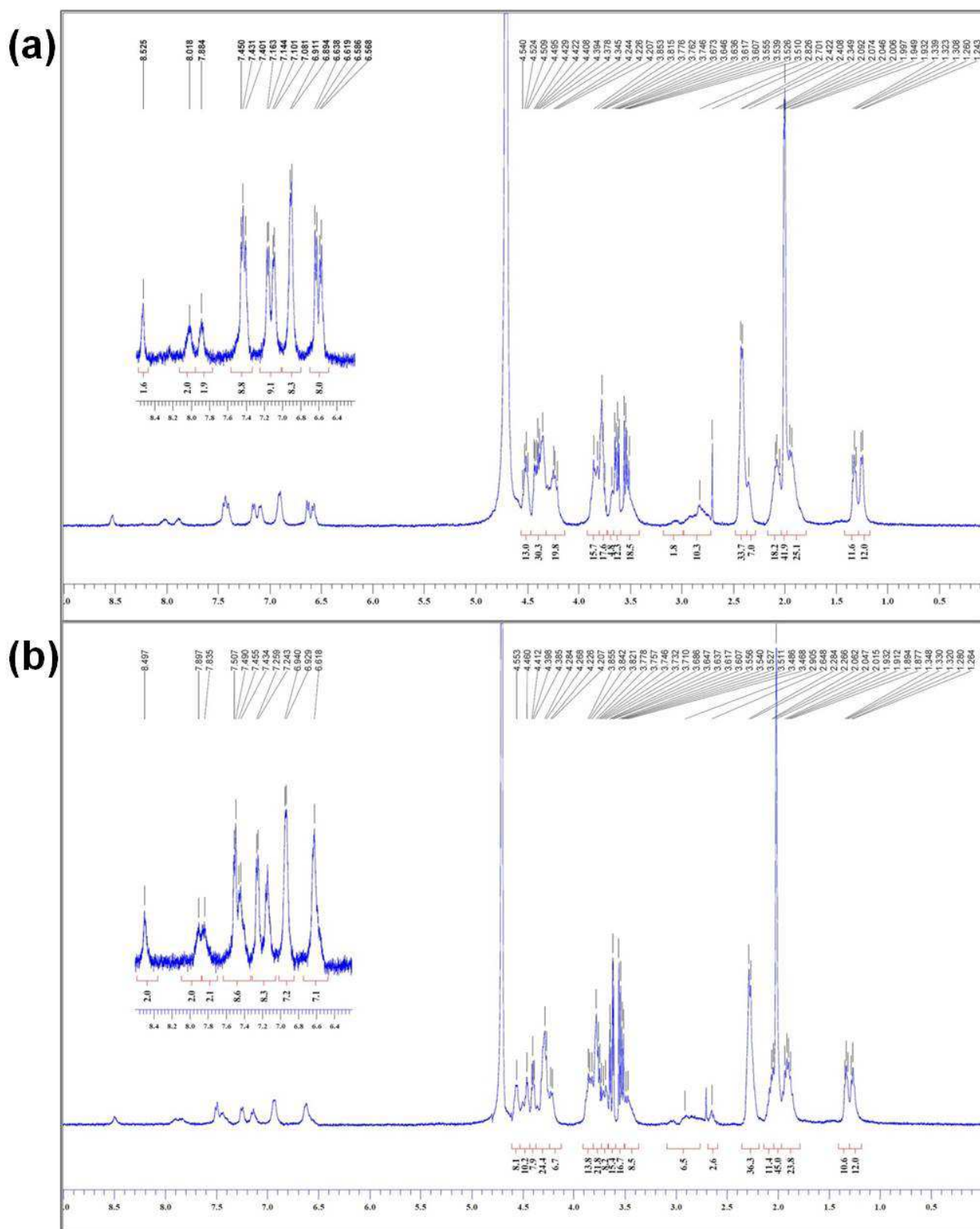
Firstly, for each Fe(II) complex, a standard 1D ¹H-NMR spectrum was acquired and evaluated to verify that the sample was diamagnetic (absence of paramagnetic line broadening and shifts).

For the diffusion experiment the standard Bruker pulse program, ledbp2s, employing longitudinal eddy current delay (LED), a bipolar gradient pulse pair, and 2 spoil gradients was utilized. Rectangular gradients with a total duration (δ) of 4-6 ms were used. The LED delay was 5 ms. Gradient recovery delays were 200 µs. Diffusion times Δ were 125-150 ms. Measurements were performed at 30.0°C.

The program Bruker Topsin 3.0b was used for data treatment. Individual rows of the 25-40 quasi-2-D diffusion databases were phased and baseline corrected, then NMR signals were integrated manually, thus defining several (15-30) points for fitting the diffusional decay according to (3), where γ is a constant (γ = 4258 G⁻¹s⁻¹) and G is the gradient strength.

$$(3) I = I_0 \cdot e^{-D \cdot (\gamma \delta G)^2 \cdot (\Delta - \delta/3) \cdot 10^4}$$

For each integral i, the program calculated a fitted decay curve and the related diffusion coefficient D_i. The curves were visually inspected to verify fitting quality and averaged diffusion coefficients D were calculated. Hydrodynamic radii r_h were obtained from the diffusion coefficients through the Stokes-Einstein relationship (D = k_BT/(6πηr_h), with η = 1.095·10⁻³ Pa·s, viscosity of D₂O at 30°C).



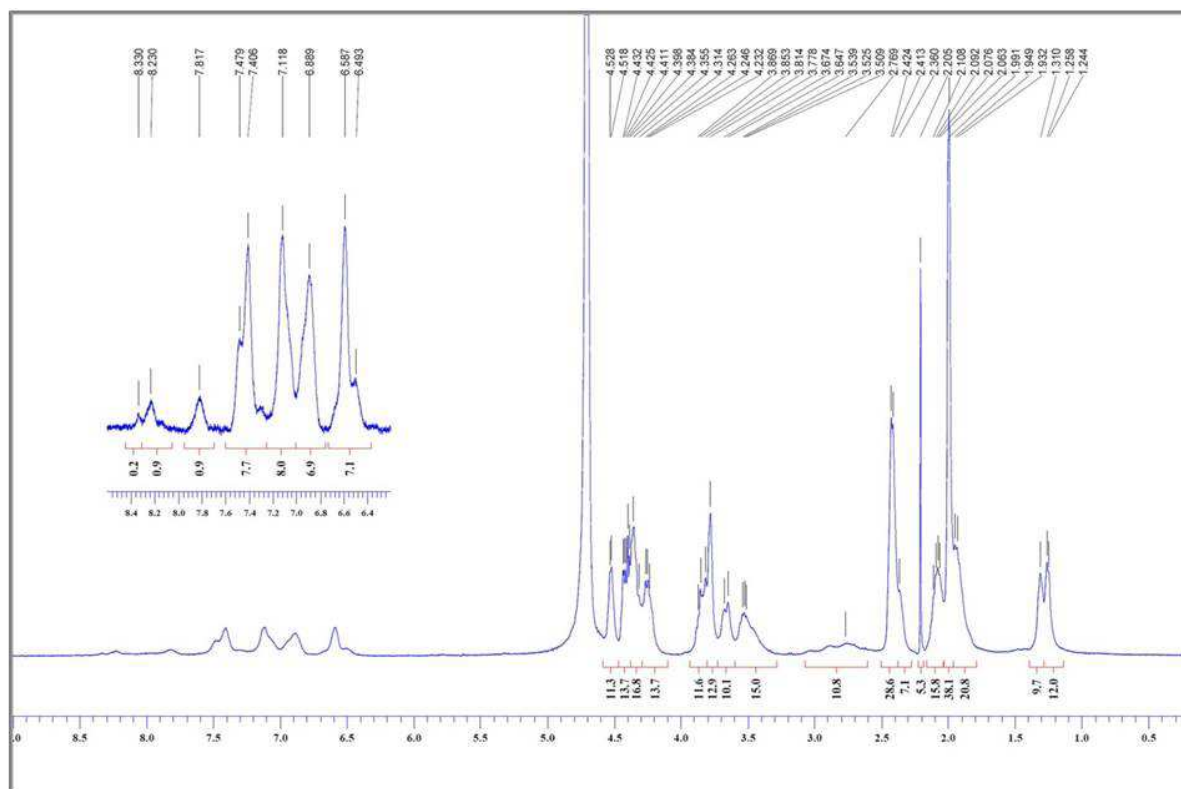


Figure S30. ^1H -NMR spectrum (400 MHz) of **BP1** 0.9 mM in D_2O + NaOD, pH 4.0, after addition of 0.30 eq $\text{Fe}(\text{NH}_4)_2(\text{SO}_4)_2 \cdot 6\text{H}_2\text{O}$. The inset shows the aromatic portion of the spectrum.

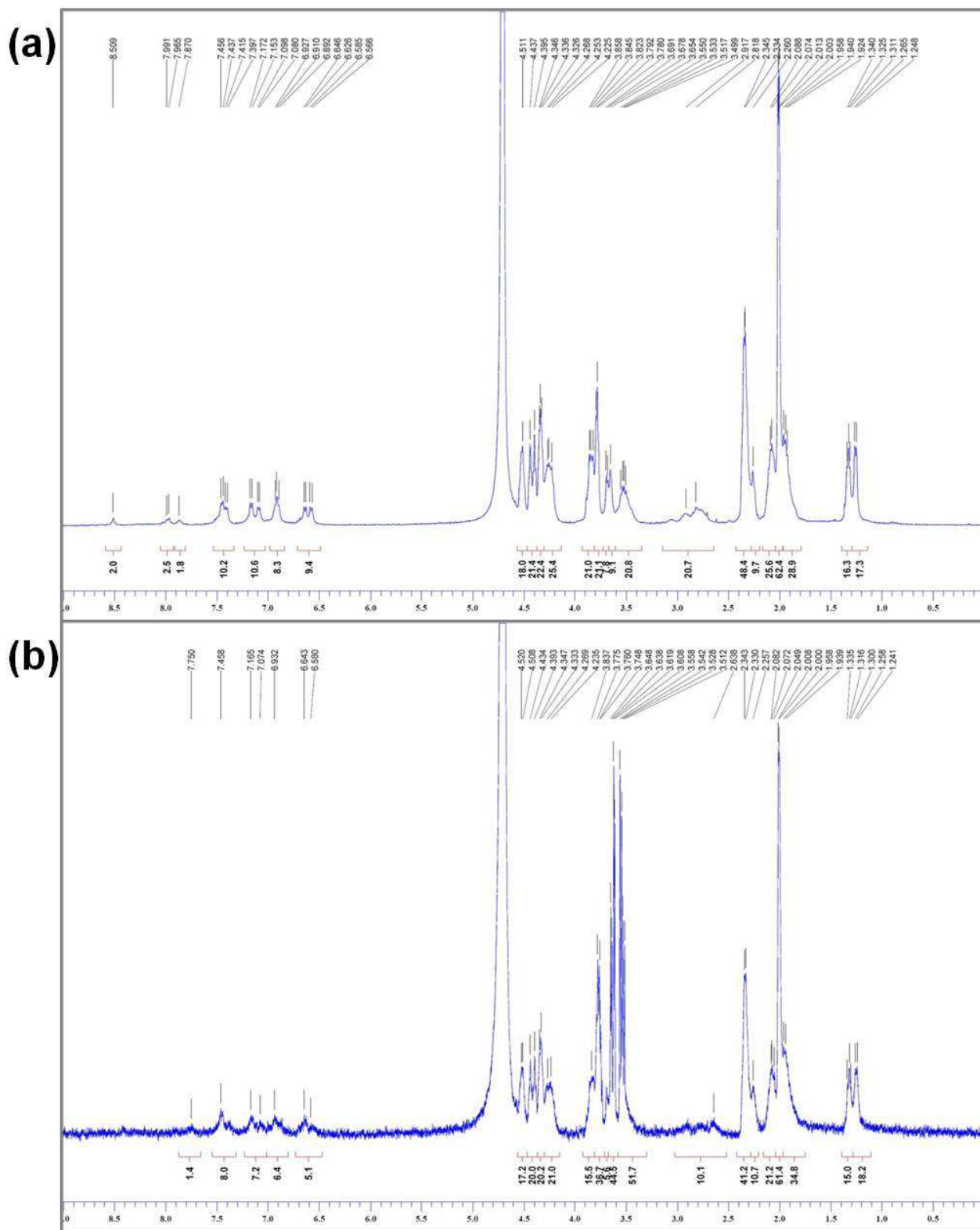


Figure S31. ^1H -NMR spectra (400 MHz) of **BP3** 0.3 mM in D_2O + NaOD, pH 4.0 (a) and pH 6.5 (b).

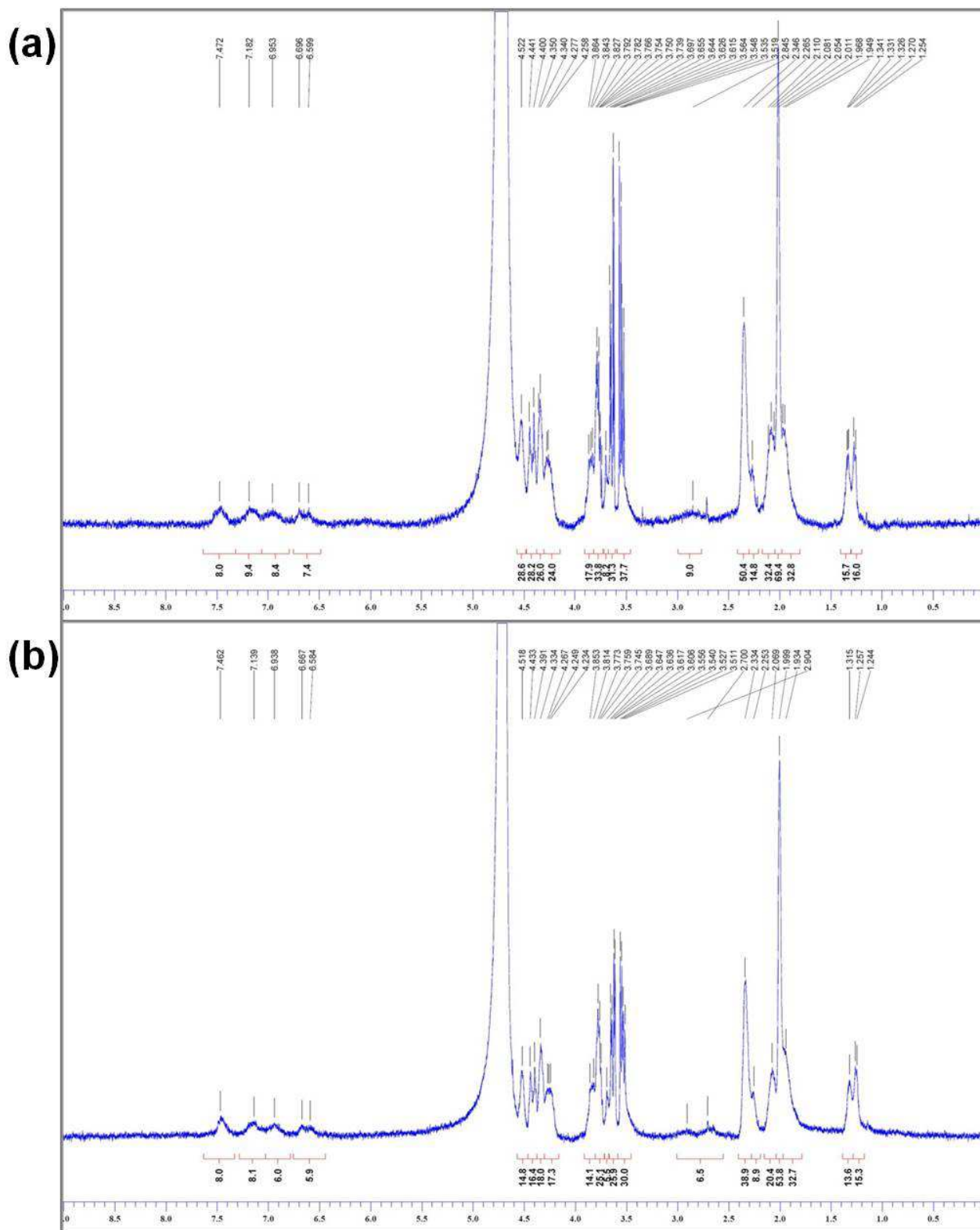


Figure S32. ^1H -NMR spectra (300 MHz) of BP3 0.3 mM in $\text{D}_2\text{O} + \text{NaOD}$, pH 4.0 (a) and pH 6.5 (b), after addition of 0.28 eq $\text{Fe}(\text{NH}_4)_2(\text{SO}_4)_2 \cdot 6\text{H}_2\text{O}$.

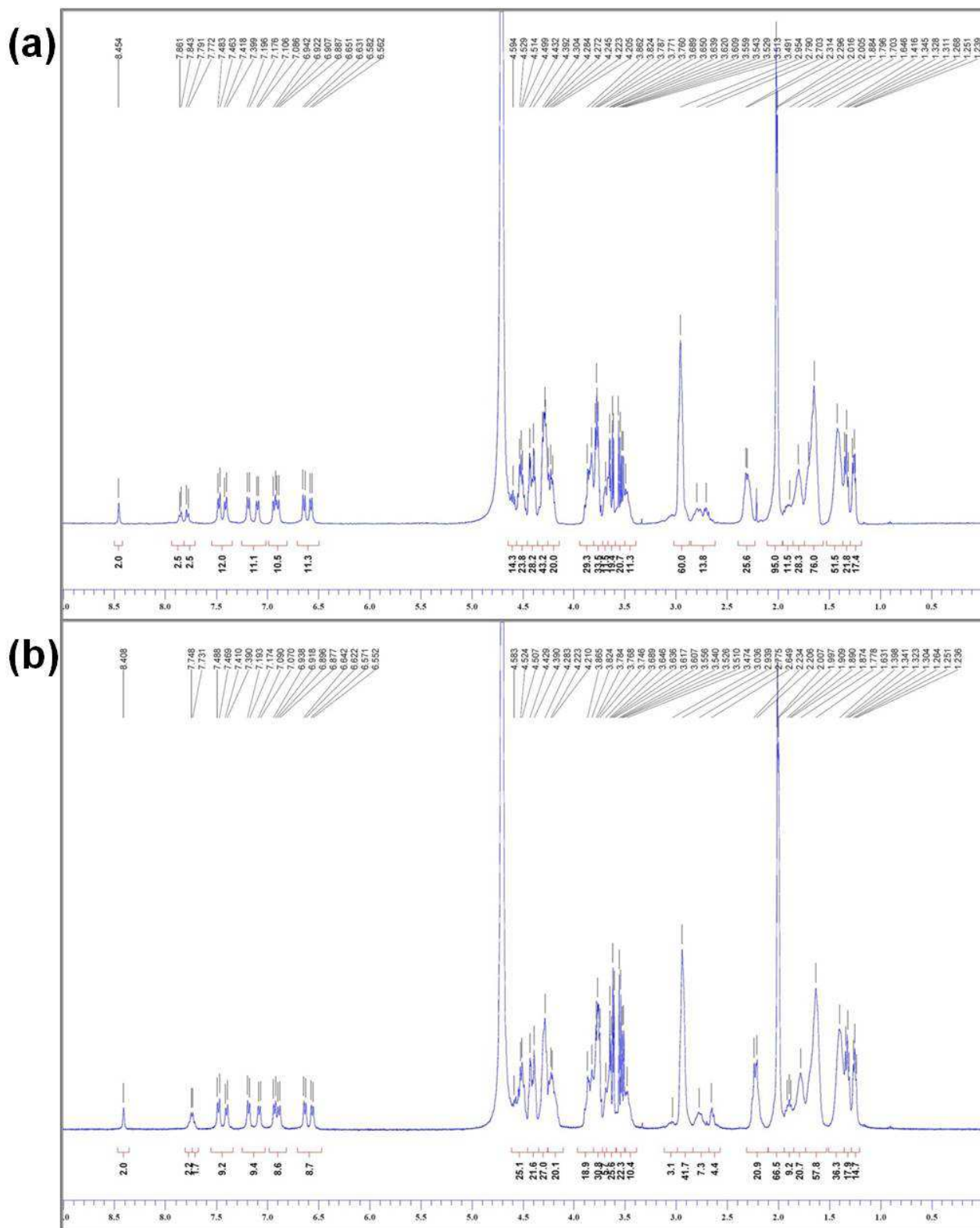


Figure S33. ^1H -NMR spectra (300 MHz) of **BP4** 0.8 mM in D_2O + NaOD, pH 4.0 (a) and pH 6.5 (b).

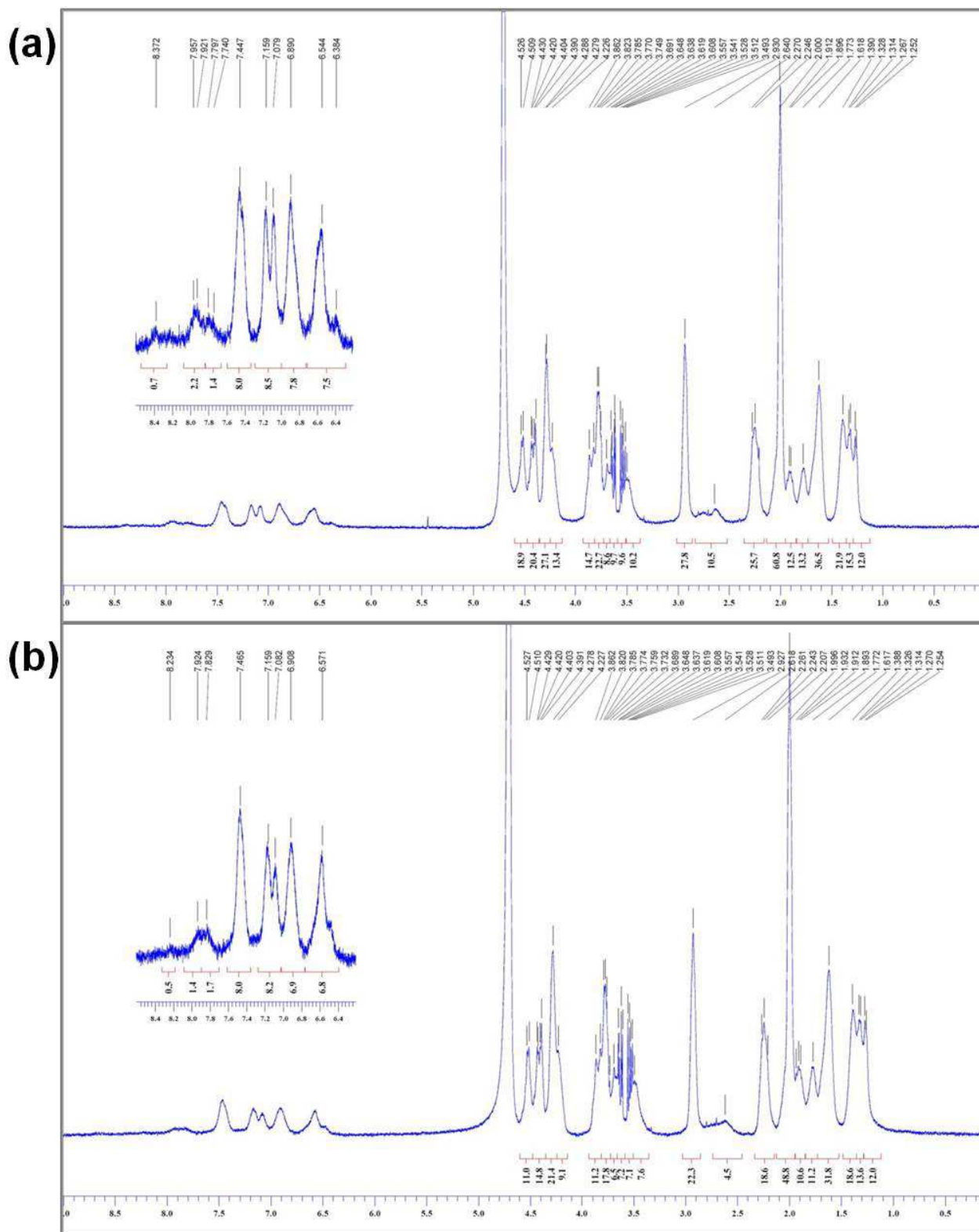


Figure S34. ¹H-NMR spectra (300 MHz) of the 2:1 mixture of BP4 and BP1, total concentration 0.65 mM in D₂O + NaOD, pH 6.5 (a) and of the same mixture plus 0.29 eq Fe(NH₄)₂(SO₄)₂·6H₂O (b). Insets show the aromatic portions of the spectra.

Circular dichroic (CD) measurements

Freshly prepared solutions of 3:1 bipyridine peptide dendrimer/Fe(II) complexes (identified by the presence of the characteristic MLCT visible band in the corresponding spectrophotometric titration) 25-50 μM in the appropriate buffer (AcONa buffer, pH 4.0, or HEPES buffer, pH 6.5) were tested, as well as 50 μM solutions of **BP1** in both buffers and of the 1:1 **BP1**/Fe(II) complex in HEPES buffer. The two buffers were used as blanks.

Instrumental parameters: $250 \leq \lambda/\text{nm} \leq 600$, scan speed 100 nm/min, step 0.5 nm, band width 1.0 nm, response 1.0 sec. Reduced volume 1.0 cm optical path quartz cells thermostated at 25.0°C were employed. 6-8 scans were recorded and averaged for each sample. After subtraction of the appropriate blank, circular dichroic signals (ΔA) were converted into total molar ellipticities ($[\Theta]_T$) and the spectra were smoothed.

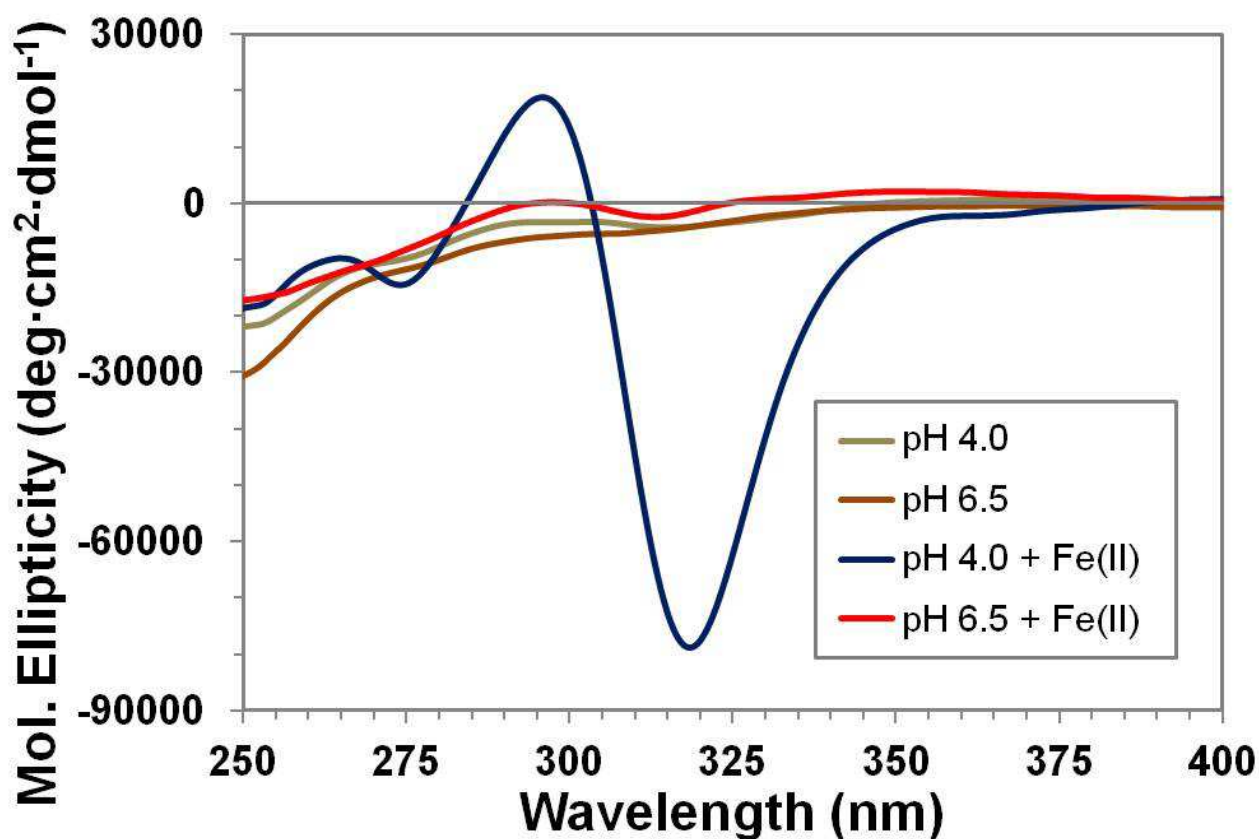
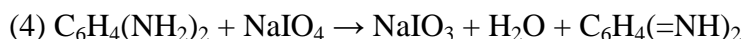


Figure S35. CD spectra of **BP1** and of its Fe(II) complexes (both 50 μM in ligand, at the pH given) in the spectral region of the bipyridyl chromophore. Solutions at pH 4.0 were prepared in AcONa buffer, solutions at pH 6.5 were prepared in HEPES buffer.

Catalytic assays

Determination of the amount of oxidized substrate

ortho-Phenylenediamine (OPD) is quantitatively oxidized by NaIO₄ according to the stoichiometry of eq. (4):



The (colorless) quinone imine product reacts further with the unreacted substrate to give a colored substance with an absorption maximum close to 425 nm; after longer standing such colored substance begins to polymerize and polymers precipitate over time.

To verify that the absorbance of the colored substance at 425 nm was proportional to the amount of oxidized OPD and to obtain the proportionality constant the following experiment was performed.

OPD (1.63 mg, 14.8 μmol) was dissolved in 3.69 mL 20 mM HEPES buffer, pH 6.5, purged with argon, yielding a 4.0 mM solution. Aliquots of the mother solution were diluted with the same buffer to prepare a 1.0 mM and a 0.4 mM daughter solution. The required amounts of the three solutions were pipetted into the wells of a microtiter plate and buffer was added, so that four rows of 12 wells containing 60 μL of OPD solutions at 0–3.3 mM concentration were prepared.

NaIO₄ (6.95 mg, 31.8 μmol) was dissolved in 1.59 mL milliQ H₂O purged with argon, yielding a 20 mM mother solution. Aliquots of the mother solution were diluted with milliQ H₂O to prepare a 10 mM and a 5 mM daughter solution.

After reading the plate, 2 μL aliquots of the 5, 10, 20 mM NaIO₄ solutions were added to each well of the first, second, third row, respectively, whereas the wells of the fourth row were used as a control. After shaking gently for 10 min at 25.0°C the plate was read. The NaIO₄ addition was repeated five more times with the same procedure.

For each well the absorbance at λ 425 nm in the six readings was plotted and graphs were built comparing the wells within the same row. No significant variation among the readings was observed for the wells of the control row. On the contrary, within each of the three other rows, all wells displayed the same linear increase with negative deviations from linearity as the amount of added NaIO₄ increased (Figure S36a).

UPLC analyses showed the complete disappearance of the substrate peak from the wells which had reached a plateau (Figure S37), thus confirming the hypothesis of quantitative oxidation.

Since the oxidation is quantitative and the linearity of the first portion of the graph supports a linear proportionality between measured absorbance, A_{(OPD(ox))}, and concentration of oxidized substrate (c_{(OPD)ox}), it is possible to write eq. 5 according to the Lambert-Beer law:

$$(5) A_{(\text{OPD}(\text{ox}))} = \epsilon b c_{(\text{OPD})\text{ox}}$$

Considering the experimental setup (cylindrical, flat-bottomed wells), the optical path *b* is proportional to the solution volume. For a given amount of oxidized substrate in a well (n_{OPD(ox)}), the concentration is inversely proportional to the solution volume and therefore also to the optical path, so that the absorbance is dilution insensitive, depending only on the amount of oxidized substrate. The relationship between absorbance and oxidized substrate amount is expressed in eq. (6).

$$(6) A_{(\text{OPD}(\text{ox}))} = b n_{(\text{OPD})\text{ox}} \quad [n_{(\text{OPD})\text{ox}} = n_{\text{OPD}(0)} \text{ by quantitative oxidation}]$$

The proportionality constant *b* is the slope of the graph of the average absorbance increase against substrate amount (Figure S36b) in its linear portion and allows one to obtain the amount of oxidized substrate in moles from the well absorbance.

Since the kinetic experiments were designed to have the same total volume of solution in each well (V_t , 105 μL), in the calculations related to such experiments it is possible to work with concentrations throughout. A proportionality constant b' referred to the concentration by the total volume V_t can therefore be defined and obtained from eq. (7).

$$(7) \quad b n_{(\text{OPD})_{\text{ox}}} = b(c_{(\text{OPD})_{\text{ox}}} V_t) = b' c_{(\text{OPD})_{\text{ox}}} \quad b' = b V_t = 2.547 \pm 0.053 \text{ mM}^{-1}$$

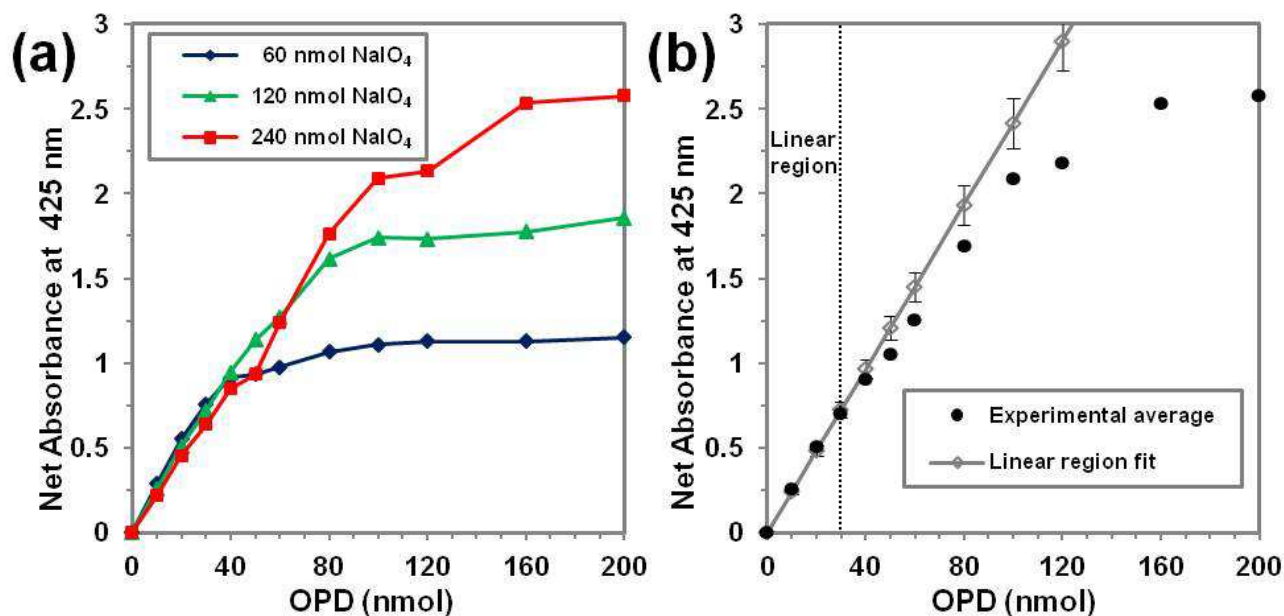


Figure S36. (a) Maximum absorbance increase at λ 425 nm by oxidation of OPD with different amounts of NaIO₄ as a function of the substrate amount. (b) Fitting of the averaged experimental results according to the relationship $A = b n_{(\text{OPD})_{\text{ox}}}$ based on the linear region of the graph (oxidized OPD ≤ 30 nmol, corresponding to $A \leq 0.7$). Error bars represent the uncertainty in the proportionality constant b ($0.02426 \pm 0.00050 \text{ nmol}^{-1}$).

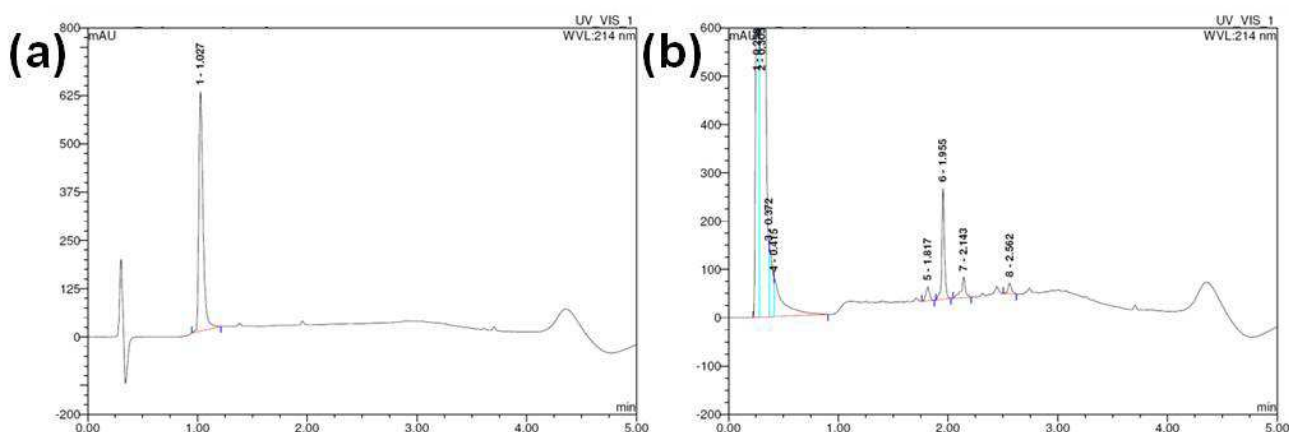


Figure S37. UPLC comparison of OPD in control well (a) and of the content of a well treated with excess NaIO₄ (b). Conditions: 50 nmol OPD in both wells, 240 nmol NaIO₄ added in b, after 1 h equilibration. Gradient: 0-30 % B in 2.2 min, λ 214 nm.

Test of oxidation catalysis

Preparation of the solutions of the Fe(II) complexes

$[\text{Fe}(\text{bipy})_3]^{2+}$: $\text{Fe}(\text{NH}_4)_2(\text{SO}_4)_2 \cdot 6 \text{H}_2\text{O}$ was freshly dissolved in milliQ H_2O under argon stream at a 1.00 mM concentration. 2,2'-bipyridine (bipy) was dissolved in milliQ H_2O at a 3.00 mM concentration. Equal volumes of both solutions were mixed under argon and the resulting solution was diluted 1:5 with milliQ H_2O , yielding a 100 μM $[\text{Fe}(\text{bipy})_3]^{2+}$ solution.

$[\text{Fe}^{\text{II}}(\text{BP1})]$: $\text{Fe}(\text{NH}_4)_2(\text{SO}_4)_2 \cdot 6 \text{H}_2\text{O}$ was freshly dissolved in milliQ H_2O under argon stream at a 1.10 mM concentration. Lyophilized **BP1** was dissolved in HEPES buffer, pH 6.5, at a concentration of 0.111 mM. 0.11 mL $\text{Fe}(\text{NH}_4)_2(\text{SO}_4)_2$ solution (1.07 eq) were mixed with 1.02 mL $\text{bipy}(\text{CH}_2\text{N1})_2$ solution, yielding 1.13 mL 100 μM $[\text{Fe}^{\text{II}}(\text{BP1})]$ solution.

Both solutions were freshly prepared shortly before the kinetic experiment.

Experimental setup

A 4.0 mM mother solution of OPD and 1.0 mM, 0.4 mM diluted solutions were prepared in HEPES buffer, pH 6.5, as described in the preceding section. A 100 μM solution of Fe(II) source ($\text{Fe}(\text{NH}_4)_2(\text{SO}_4)_2 \cdot 6 \text{H}_2\text{O}$ or one of the complexes described above) was prepared.

The required amounts of the three substrate solutions and of HEPES buffer were pipetted into the wells of a microtiter plate so that one control row and two sample rows of 12 wells each with 0–200 nmol OPD in 65 (control row) or 60 (sample rows) μL solution were obtained. 40 μL 10 mM H_2O_2 (freshly prepared by dilution of 30 % H_2O_2 with milliQ H_2O) were added to each well and the plate was mixed thoroughly. 5 μL 100 μM Fe(II) source solution were rapidly added to the two sample rows (starting from the wells containing the smallest amount of substrate) and the plate was mixed thoroughly. The plate was then kept at 25.0°C and shaken gently during 4 h, with readings at λ 425 nm every minute.

For the bipyridine-peptide dendrimer complex two independent experiments were performed.

To verify the stability of the $[\text{Fe}^{\text{II}}(\text{BP1})]$ complex under the experimental conditions, after the oxidation catalysis test a microtiter well solution prepared from 40 μL 10 mM H_2O_2 and 5 μL 100 μM $[\text{Fe}^{\text{II}}(\text{BP1})]$ in 60 μM 20 mM HEPES buffer was analyzed by UPLC (Fig. S38a) and compared with the 100 μM $[\text{Fe}^{\text{II}}(\text{BP1})]$ mother solution (Fig. S38b).

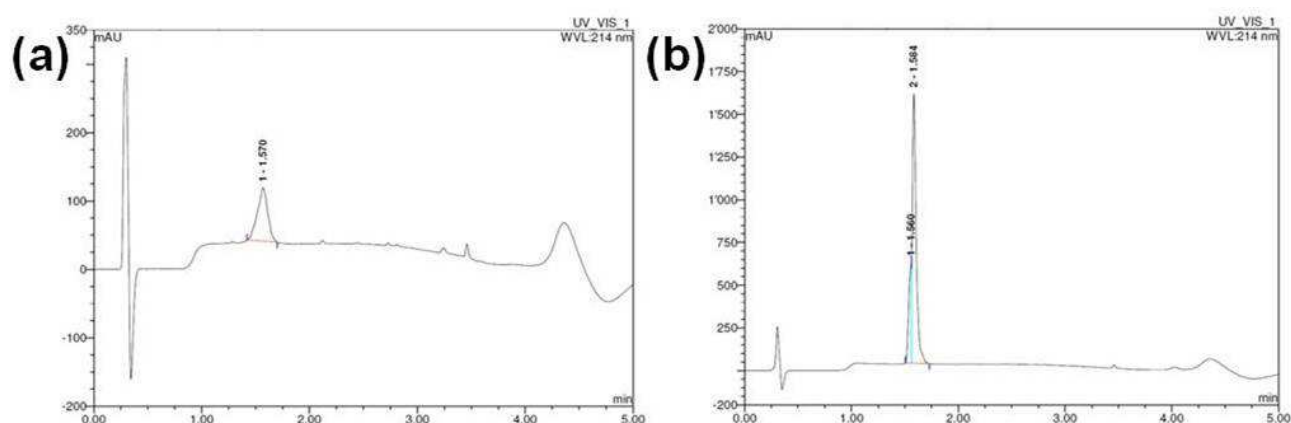


Fig. S38. UPLC comparison of 4.8 μM $[\text{Fe}^{\text{II}}(\text{BP1})]$ in 12 mM HEPES buffer, pH 6.5, after 4 hours treatment with 3.9 mM H_2O_2 (a) and of the 100 μM $[\text{Fe}^{\text{II}}(\text{BP1})]$ mother solution. . UPLC conditions: Dionex UPLC, gradient 0 - 70 % B in 2.2 min, λ 214 nm.

Data treatment

Conversion graph, relative conversion, TON, TOF data

For each well, a graph of the absorbance increment was prepared by subtracting the initial reading from all data. The graph was transformed into a conversion graph through the proportionality constant b' obtained as described in the preceding section. After smoothing all series independently, the average conversion for each set of experimental conditions (Fe(II) source and substrate concentration) was calculated, as well as the related uncertainty. Net conversion data for the series of the three Fe(II) sources were obtained by subtracting the conversion values of the control series at a given initial substrate concentration from the total conversion data at the same initial substrate concentration. From the original graph, consisting of 241 time points for 48 series (12 substrate concentrations for the three Fe(II) sources and the control data), a simplified graph displaying conversion at selected times for the most concentrated series for each Fe(II) source and for the control experiment was prepared (Figure 4a in the main text).

Total relative conversion and net relative conversion data were obtained for each series by dividing the corresponding total conversion and net conversion data by the initial substrate concentration. A graph of the maximum net relative conversion as a function of substrate concentration was prepared (Figure S39). Net turnover number (TON) data were obtained by dividing the corresponding net conversion data at selected reaction times (10, 20, 30 min, as well as 1, 2, 3, 4 h) by the initial concentration of the Fe(II) source (Table S7). A net TON graph was prepared by plotting net TON data as a function of substrate concentration at selected times (Figure S40a). Net turnover frequency (TOF) data were obtained by dividing the corresponding net TON data by the reaction time. A net TOF graph was prepared by plotting net TOF values as a function of substrate concentration at selected times (Figure S40b).

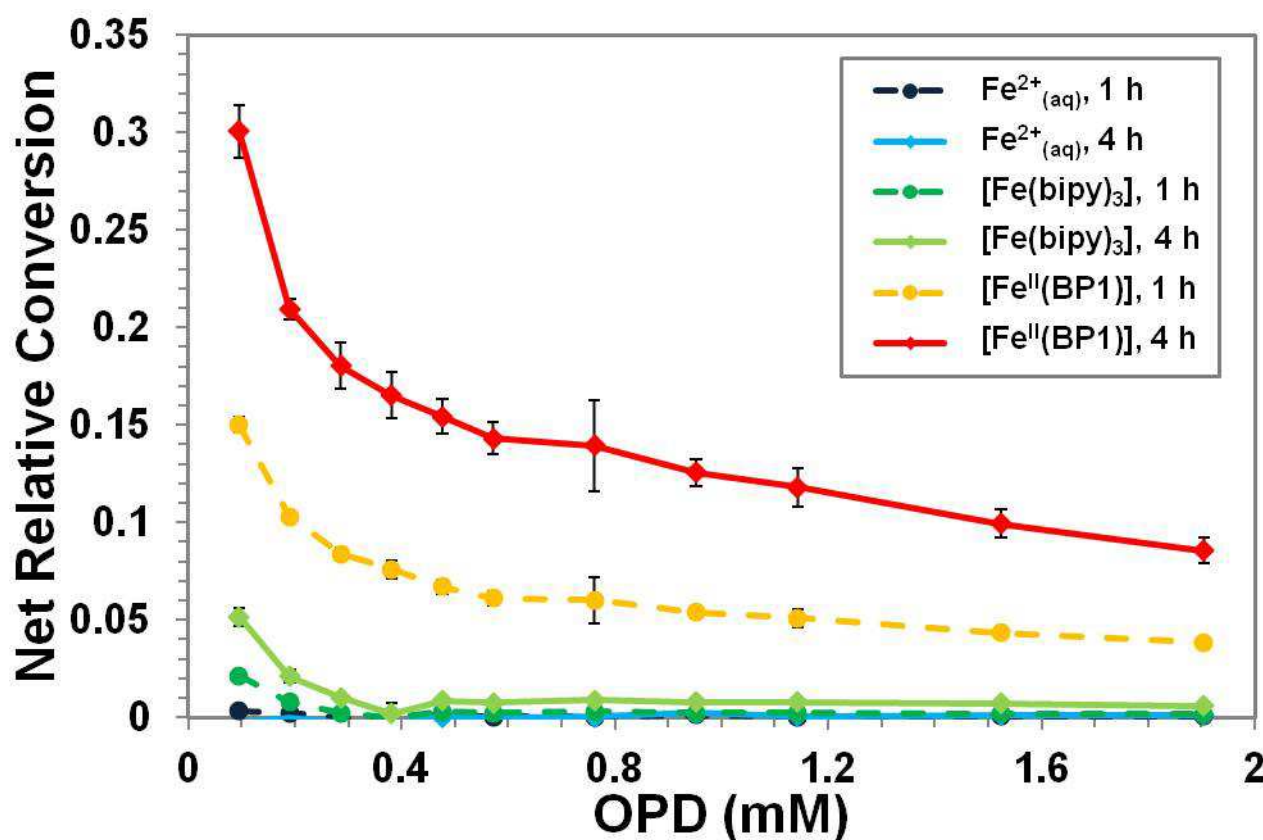


Figure S39. Net relative conversion of the substrate for OPD oxidation by H_2O_2 as a function of its initial concentration for the three Fe(II) sources tested as catalysts after 1 and 4 hours. Conditions: substrate 0.095 – 1.9 mM, H_2O_2 3.9 mM, Fe(II) source 4.8 μM , pH 6.5 (HEPES buffer 12 mM), 25°C.

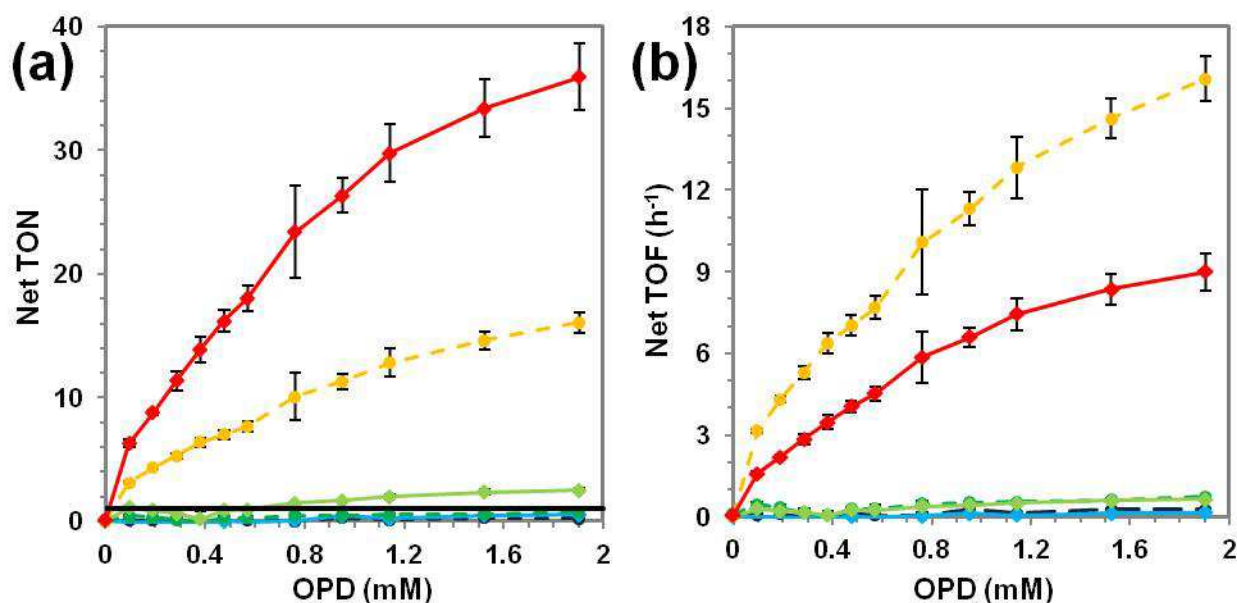


Figure S40. Net turnover number (TON, a) and net turnover frequency (TOF, b) for OPD oxidation by H_2O_2 as a function of its initial concentration for the three Fe(II) sources tested as catalysts after 1 and 4 hours. The same color coding was used as in Figure S39. The black bar in (a) corresponds to stoichiometric conversion (TON = 1). Conditions: substrate 0.095 – 1.9 mM, H_2O_2 3.9 mM, Fe(II) source 4.8 μM , pH 6.5 (HEPES buffer 12 mM), 25°C.

Table S7. Net TONs for the Oxidation of OPD by H_2O_2 in the Presence of Different Fe(II) Sources^a

cOPD ₀ (mM)	0.095	0.19	0.29	0.38	0.48	0.57	0.76	0.95	1.14	1.52	1.91
$\text{Fe}^{2+}_{(\text{aq})}$, 10'	0.011	0.068	0.021	0.001	0.104	-0.004	0.020	0.103	0.081	0.074	0.125
$\text{Fe}^{2+}_{(\text{aq})}$, 20'	0.034	0.084	0.013	-0.031	0.128	-0.016	0.012	0.168	0.088	0.114	0.154
$\text{Fe}^{2+}_{(\text{aq})}$, 30'	0.050	0.108	0.013	-0.050	0.118	-0.011	0.007	0.207	0.105	0.183	0.181
$\text{Fe}^{2+}_{(\text{aq})}$, 1 h	0.068	0.095	-0.019	-0.078	0.128	0.051	0.035	0.256	0.114	0.256	0.252
$\text{Fe}^{2+}_{(\text{aq})}$, 2 h	0.030	0.078	-0.101	-0.140	0.140	0.021	0.036	0.314	0.116	0.318	0.325
$\text{Fe}^{2+}_{(\text{aq})}$, 3 h	-0.009	0.035	-0.145	-0.213	0.077	-0.006	0.048	0.389	0.157	0.403	0.454
$\text{Fe}^{2+}_{(\text{aq})}$, 4 h	-0.054	-0.010	-0.188	-0.279	0.020	-0.012	0.066	0.455	0.200	0.474	0.549
$[\text{Fe}(\text{bipy})_3]$, 10'	0.061	0.072	-0.014	-0.006	0.075	0.035	0.012	0.137	0.047	0.104	0.211
$[\text{Fe}(\text{bipy})_3]$, 20'	0.165	0.154	0.010	-0.001	0.120	0.095	0.083	0.238	0.136	0.225	0.344
$[\text{Fe}(\text{bipy})_3]$, 30'	0.232	0.200	0.034	-0.024	0.175	0.128	0.161	0.268	0.218	0.346	0.426
$[\text{Fe}(\text{bipy})_3]$, 1 h	0.452	0.336	0.144	-0.020	0.294	0.292	0.471	0.510	0.533	0.611	0.724
$[\text{Fe}(\text{bipy})_3]$, 2 h	0.697	0.547	0.358	0.053	0.647	0.578	0.758	0.905	1.014	1.258	1.450
$[\text{Fe}(\text{bipy})_3]$, 3 h	0.908	0.730	0.528	0.090	0.770	0.789	1.153	1.334	1.563	1.862	2.044
$[\text{Fe}(\text{bipy})_3]$, 4 h	1.083	0.882	0.634	0.175	0.895	0.970	1.471	1.674	1.986	2.369	2.522
$[\text{Fe}^{\text{II}}(\text{BP1})]$, 10'	0.858	1.234	1.493	1.776	1.978	2.138	2.808	3.171	3.609	4.088	4.402
$[\text{Fe}^{\text{II}}(\text{BP1})]$, 20'	1.507	2.124	2.578	3.077	3.378	3.676	4.820	5.394	6.120	6.981	7.546
$[\text{Fe}^{\text{II}}(\text{BP1})]$, 30'	2.007	2.822	3.419	4.084	4.476	4.871	6.395	7.119	8.102	9.286	10.047
$[\text{Fe}^{\text{II}}(\text{BP1})]$, 1 h	3.152	4.317	5.284	6.372	7.026	7.686	10.087	11.302	12.827	14.625	16.092
$[\text{Fe}^{\text{II}}(\text{BP1})]$, 2 h	4.544	6.430	8.014	9.376	10.747	11.653	14.982	16.659	18.846	21.827	23.812
$[\text{Fe}^{\text{II}}(\text{BP1})]$, 3 h	5.716	7.659	9.495	11.460	13.143	14.577	19.145	21.356	24.331	27.362	30.236
$[\text{Fe}^{\text{II}}(\text{BP1})]$, 4 h	6.312	8.800	11.347	13.881	16.188	18.042	23.402	26.368	29.783	33.406	35.942

^a Net turnover numbers (TONs) were calculated by dividing net conversions (experimental conversion minus the conversion observed in the control experiment) at the time given by the concentration of the Fe(II) source. The associated uncertainties are in the ranges 0.03-0.3 for $\text{Fe}^{2+}_{(\text{aq})}$, 0.03-0.6 for $[\text{Fe}(\text{bipy})_3]$ and 0.04-2.7 for $[\text{Fe}^{\text{II}}(\text{BP1})]$, growing both from shorter to longer reaction times and from lower to higher substrate concentrations. Conditions: Fe(II) source 4.8 μM , H_2O_2 3.9 mM, pH 6.5 (HEPES buffer 12 mM), 25°C.

Reaction velocity graph, pseudo-first order rate constant

For each series, a graph of the velocity of the absorbance variation was prepared by dividing the absorbance increment with respect to the first reading of each series by the experimental time. The graph was transformed into a total reaction velocity graph through the proportionality constant b' as described above. After smoothing all series independently, the average reaction velocity for each set of experimental conditions was calculated, as well as the related uncertainty. Net reaction velocity data for the series of the three Fe(II) sources were obtained by subtracting the velocity data of the control series at a given initial substrate concentration from the total reaction velocity data at the same initial substrate concentration. From the original graph, consisting of 241 time points for 48 series, a graph of the initial velocity was obtained by plotting the reaction velocity at $t = 0$ as a function of the substrate concentration for each Fe(II) source and for the control data. Similarly, a net initial velocity graph was obtained from the net reaction velocity at $t = 0$ (Figure S41a).

Total and net pseudo-first order rate constant (k') data were obtained by dividing the corresponding initial ($t = 0$) reaction velocity data by the initial substrate concentration. A graph of the net pseudo-first order rate constant as a function of the substrate concentration was plotted (Figure S41b).

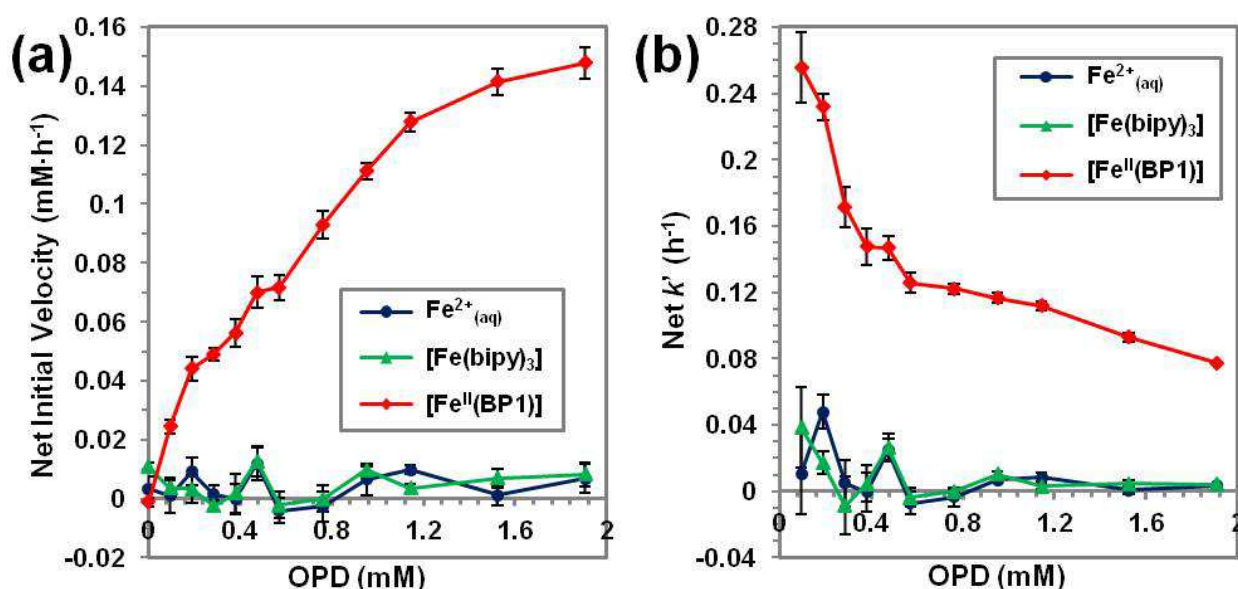


Figure S41. Net initial velocity (a) and net pseudo-first order rate constant k' (b) as a function of substrate concentration for the three Fe(II) sources tested as catalysts in OPD oxidation by H_2O_2 . Conditions: substrate 0.095 – 1.9 mM, H_2O_2 3.9 mM, Fe(II) source 4.8 μM , pH 6.5 (HEPES buffer 12 mM), 25°C.

Lineweaver-Burke graph, determination of K_M and k_{cat}

Lineweaver-Burke plots were prepared only for the $[\text{Fe}^{\text{II}}(\text{BP1})]$ series, since it was the only series displaying both catalysis ($\text{TON} > 1$) and a clear saturation trend in the net conversion graph. The reciprocal of the net initial velocity ($1/v_0$) was plotted against the reciprocal of the initial substrate concentration ($1/[\text{S}]_0$). The linear portion of this graph (Figure 4b in the main text) was fitted to eq. (8), yielding the velocity at catalyst saturation v_{max} as the inverse of the intercept (q) and K_M/v_{max} as the slope (m), whereas k_{cat} was obtained by dividing v_{max} by the concentration of the complex ($[\text{E}]$, 4.8 μM). Table S8 displays the values of the Michaelis-Menten parameters obtained from the fitting.

$$(8) \quad 1/v_0 = 1/v_{\text{max}} + (K_M/v_{\text{max}}) \cdot (1/[\text{S}]_0) \quad 1/v_0 = q + m \cdot (1/[\text{S}]_0) \quad v_{\text{max}} = k_{\text{cat}} \cdot [\text{E}]$$

Table S8. Michaelis-Menten Parameters for the [Fe^{II}(**BP1**)]-Catalyzed OPD Oxidation by H₂O₂^a

$K_M \pm sK_M$ (mM) ^b	$v_{\max} \pm sv_{\max}$ (μM·s ⁻¹) ^b	$k_{\text{cat}} \pm sk_{\text{cat}}$ (s ⁻¹) ^c	$k_{\text{cat}}/K_M \pm s(k_{\text{cat}}/K_M)$ (s ⁻¹ ·mM ⁻¹) ^d
1.51 ± 0.19	0.0776 ± 0.089	0.0163 ± 0.0019	0.01081 ± 0.00053

^a Results are given after subtraction of control contribution. ^b K_M/v_{\max} and v_{\max} were obtained from the Lineweaver-Burke double reciprocal plot. ^c k_{cat} was obtained by dividing v_{\max} by the concentration of [Fe^{II}(**BP1**)]. ^d k_{cat}/K_M was obtained by dividing the reciprocal of K_M/v_{\max} by the concentration of [Fe^{II}(**BP1**)]. Conditions: [Fe^{II}(**BP1**)] 4.8 μM, substrate 0.095 – 1.9 mM, H₂O₂ 3.9 mM, pH 6.5 (HEPES buffer 12 mM), 25°C.

References for Supplementary Information

[S1] Remote control of bipyridine–metal coordination within a peptide dendrimer. N. A. Uhlich, P. Sommer, C. Bühr, S. Schürch, J.-L. Reymond, T. Darbre, *Chem. Commun.* **2009**, 6237–6239.

[S2] Structure and Binding of Peptide-Dendrimer Ligands to Vitamin B12. N. A. Uhlich, A. Natalello, R. U. Kadam, S. M. Doglia, J.-L. Reymond, T. Darbre, *Chembiochem* **2010**, *11*, 358-365.